FABRICATION AND CHARACTERIZATION OF A PROTOTYPE PARABOLIC TROUGH SOLAR CONCENTRATOR FOR STEAM PRODUCTION

MILLIEN KAWIRA ERASTUS

MASTER OF SCIENCE

(Physics)

JOMO KENYATTA UNIVERSITY OF AGRICULTURE AND TECHNOLOGY

2011

Fabrication and Characterization of a Prototype Parabolic Trough Solar Concentrator for Steam Production

Millien Kawira Erastus

A thesis submitted in partial fulfillment for the degree of Master of Science in Physics in the Jomo Kenyatta University of Agriculture and Technology.

2011

DECLARATION

This thesis is my original work and has not been presented for a degree in any other university.

Signature…….. Date…….

Millien Kawira Erastus

This thesis has been submitted for examination with our approval as the university supervisors.

Signature:…… Date……..

Dr. Robert Kinyua

JKUAT, Kenya

Signature:…… Date:…….

Dr. J. Ngugi Kamau

JKUAT, Kenya

DEDICATION

I dedicate this work to my love Andrew, our children Patricia and Derrick, my beloved mother Beatrice, who is my model for her steadfast devotion in my education and to all my parents.

ACKNOWLEDGEMENT

This research work consists of contributions from various people. I take this opportunity to express my gratitude to my supervisors Dr. Robert Kinyua and Dr. J Ngugi Kamau for their moral, material, financial and exemplary guidance and visionary suggestions throughout the research period. I also thank them for sacrificing and being present whenever an issue arose and the expediency with which they addressed the task at hand, especially at the research site. They were a source of motivation to move to the end of this research.

We extend our appreciation to the chairman Physics Department, Dr. Ngaruiya for his support during the research, and all the members of the Physics Department for their useful contribution in various ways. We also thank all the technical staff in the Physics Department for their assistance in various ways. We would also like to thank the Mechanical Engineering Department for assisting us with some of the apparatus, and also Mr. Waweru for assisting in the fabrication of the solar concentrator. We also wish to thank the Estates Department for providing the ladder and also useful technical advice during plumbing.

Finally, I thank my beloved husband Andrew, our children Patricia and Derrick and parents for their support during the research.

TABLE OF CONTENTS

LIST OF TABLES

LIST OF FIGURES

LIST OF PLATES

LIST OF APPENDICES

LIST OF ABBREVIATIONS

ASHRAE	American society of heating refrigerating and air conditioning
CSP	Concentrated solar power
G I	Galvanized iron pipe
NBS	National bureau of standards
NREL	National Renewable Energy Laboratory
PTSC	Parabolic trough solar concentrator
SEGS	Solar energy generating station
SWERA	Solar and wind energy resource assessment

NOMENCLATURE

I_b	Incident flux beam (W/m^2)
θ	Angle between incident flux beam and normal to a plane surface (^{o})
$\emptyset$	Latitude (^{o})
θ_z	Zenith angle (^{o})
δ	Declination (^{o})
φ	Surface azimuth angle (^{o})
ω_t	Hour angle (^{o})
β	Angle of inclination or slope (^{o})
r_b	Tilt factor for beam radiation
I_T	Solar flux falling on a surface (W/ m^2)
I_d	Diffuse flux beam (W/ m^2)
$I_{\lambda s}$	Wavelength dependent specular reflected intensity (W/ m^2)
$I_{\lambda j}$	Wavelength dependent incident intensity (W/ m^2)
r_r	Radiation shape factor
CR	Concentration ratio
ρ	Spectral reflectance
I_g	Flux on a horizontal surface (W/ m^2)
F	Focal length (m)
a	Aperture (m)
$\dot{m}$	Mass flow rate (kg/s)
c_p	Specific heat capacity (J/kg^{o}C)
q_u	Concentrator useful heat gain (J)

A_c	Collector area (m^2)
T_2	Outlet temperature of heat transfer fluid (^oC)
T_1	Inlet temperature of heat transfer fluid (^oC)
$H_b r_b$	Solar flux intensity (W/ m^2)
α	Spectral absorptance
τ	Transmittance
L	Length of collector (m)
A_b	Calorimeter base
U_L	Heat loss coefficient (W/ m^2)
T_m	Mean temperature of heat transfer fluid (^oC)
A_a	Aperture area (m^2)
CA	Collector area (m^2)
γ	Intercept factor (W/ m^2)
T_a	Ambient temperature (^oC)
A_r	Area of receiver (m^2)
F'	Collector efficiency factor
S	Absorbed solar radiation (W/ m^2)
F_R	Collector heat removal factor
Q_u	Total heat gain by receiver (J/ m^2)
F''	Collector flow factor
η_c	Collector efficiency (%)
η_{opt}	Optical efficiency (%)
I_{max}	Maximum flux density (W/ m^2)

$\mathbf{I}(\boldsymbol{\omega})$	Radiation flux density (W/ m^2)
$\boldsymbol{\omega}$	Distance from the center of zone of solar image (m)
$\boldsymbol{w}$	Half width aperture of concentrator (m)
$\boldsymbol{h}$	Normal flux distribution coefficient (W/m)
$\boldsymbol{\sigma}$	Standard deviation of the normal distribution curve (m^2/W)
$\boldsymbol{I}$	Radiative flux density at radial position from axis r/R (W/ m^2)
$\boldsymbol{r}$	Radius in focal plane from axis (m)
$\boldsymbol{R}$	Rim radius of concentrator (m)
$\boldsymbol{D_i}$	Internal diameter of absorber (m)
$\boldsymbol{D_o}$	Outer diameter or absorber (m)
$\boldsymbol{C}$	Heat transfer thermal capacity per square meter (J/^{o}C)
$\boldsymbol{c_f}$	Specific heat capacity of heat transfer fluid (J/ kg ^{o} C)
$\boldsymbol{\emptyset_r}$	Rim angle of concentrator (^{o} C)
$\dot{\boldsymbol{Q}}_{\boldsymbol{elec}}$	Rate of electricity power use (W/ s)
$\boldsymbol{\lambda}$	Wavelength (m)
$\boldsymbol{\varepsilon}$	Emissivity
$\boldsymbol{\Delta f}$	Energy increment (J)
$\boldsymbol{P}$	Pressure (N/m^2)
$\boldsymbol{TC}$	Collector chamber temperature (^{o}C)
$\boldsymbol{m}$	Mass (kg)
$\boldsymbol{Q_{av}}$	Average heat absorbed by receiver (J)
$\boldsymbol{A_s}$	Surface area (m^2)

η_{opt} Optical efficiency (%)

r_r Rim radius (m)

ABSTRACT

Parabolic trough solar concentrators (PTSC) are gaining acceptance as transducers for renewable energy from the sun. During production of power using PTSC's no green house gases are produced. In this work parabolic trough solar concentrators for steam production made from appropriate materials were designed, fabricated and characterized. Appropriate materials considered in this work are locally available. The appropriate materials that were tested were aluminium sheet, car solar reflector and aluminium foil. Concentrators made from these materials produced efficiencies which compared favorably with the ones made from selective materials and automatically tracked; aluminium sheet 54.65 %, car solar reflector 53.16 % and aluminium foil 49.26 %. These results were lower than for Luz collector 68 %, Euro trough 65.2% and the sky fuel 73%. The highest temperature of heat transfer fluid obtained was 248.3 ^{o}C Therefore these fabricated concentrators can provide green power which would reduce amount of green house gases produced. Current research in the area of parabolic trough solar concentrators is on reducing the cost of concentrator and making it more effective and consequently delivering electrical power at lowest possible cost. Towards this end, parabolic trough solar concentrators were fabricated by use of appropriate materials that are readily available and affordable. The use of common mathematical expressions in the design demystifies the PTSC technology of design by localizing the design activities. In this work, heat losses from the receiver have been reduced by having it in the interior of the concentrator, due to the stagnant air imposed between the receiver and its cover. Modified collector testing loop with reference to ASHRAE-

93-77 was applied in collector testing. Among other procedures used were calorimetric determination of intercept factor, overall heat loss coefficient and temperature control e.t.c. Use of automatic more precise tracking system, evacuated receiver tube and use of selective coatings made the efficiencies of documented PTSC higher than for the ones that were locally fabricated.

CHAPTER ONE

INTRODUCTION

1.1 Background

Solar energy falls under the category of renewable energy sources. Renewable energy sources are energy sources that do not cause pollution and global warming to the environment. Fossil fuels give out carbon dioxide and water vapor emissions which are major contributors to global warming. Renewable energy is energy obtained from natural resources free of charge including sunlight, wind, rain, tides and geothermal heat which are naturally replenished. Fossil fuel could be understood to be transitional sources in this context. Solar energy cannot be depleted in a time relevant to human race. Sustainable energy is one which in its production and consumption has minimum counter effects on living things and the environment and is in continuous supply. Solar energy is classified as green energy since it is a source of energy that is environmentally friendly and non- polluting. Figure 1.1 shows quantities of some fossil fuel resources remaining with usual usage.

Due to concerted efforts towards environmental conservation, many governments are emphasizing power generation from renewable and alternative sources of energy. The sun is the main source of energy and hence solar technologies have significant potential to provide electricity without polluting the environment. Although coal, oil and gas provide affordable energy, incentives in developing solar technologies are becoming more feasible, reliable and profitable technology (Arnold, 2010).

Parabolic trough solar thermal power technology is the most widely accepted solar thermal conversion among the three solar thermal technologies (Price, *et al*, 2010)

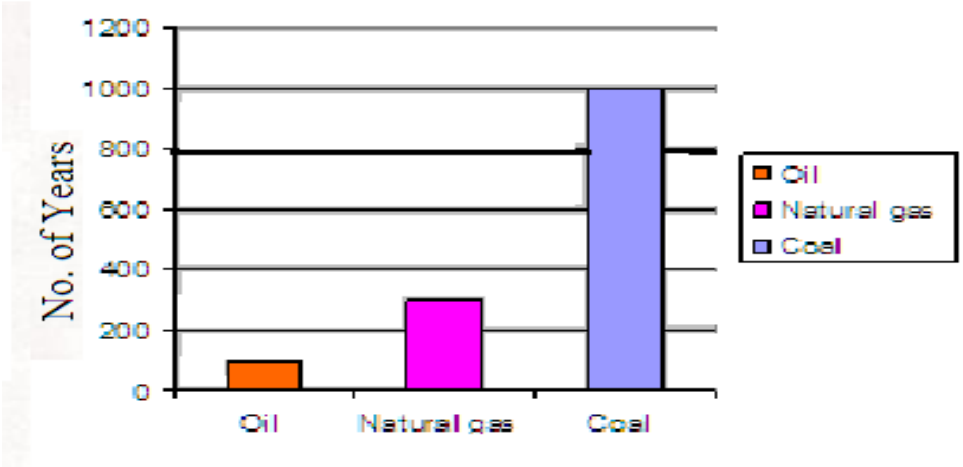

Figure 1.1: Years of left oil, natural gas and coal resources. (UNDP, 2002)

Solar thermal energy is the energy from the sun that is absorbed by a heat transfer fluid circulating in a receiver of a solar concentrating system. It is transmitted in form of electromagnetic waves from the sun. Thermal efficiency of a solar concentrating system is the percentage of absorbed energy from the sun's incident beam that is used to produce electricity.

1.2 Solar concentrators

Solar flux must be concentrated to a point or a linear axis to achieve high temperatures of heat transfer fluid. Also the efficiency of heat engine used increases the output temperature of the heat transfer fluid. The incident solar flux is concentrated by solar collectors onto a receiver which transmits thermal energy to heat transfer fluid. The high temperature steam or air produced from the receiver through a heat exchanger to the turbine rotates the shaft of a generator producing

power. To generate power from the sun, due to its low energy density, a wide area for harnessing solar flux is used.

The main commercially available concentrated solar power (CSP) technologies are parabolic trough, central power towers and parabolic dish systems. The heat transfer fluids used in these systems include synthetic oils, molten salts and pressurized steam or air.

Parabolic trough systems are long reflectors of parabola cross section with a receiver fixed at the focal axis. The mirrors of parabolic shape focus the sun's image on the receiver, which transmits thermal heat energy to the heat transfer fluid. Receiver tubes are usually made of copper or steel coated with selective coatings. In some collectors the surrounding area of receiver is evacuated to reduce heat losses. The trough tracks the sun on a single axis.

The central power towers consists of flat heliostat mirrors which focus incident solar flux on a centrally located receiver. The mirrors have a tracking system and they automatically follow the sun. Each mirror has its own dual axis control. The receiver transfers thermal heat energy to a heat transfer fluid which is used to produce high temperature steam and operate a convectional power cycle. The efficiency of the system increases with the temperature of the heat transfer fluid. In order to achieve high temperatures molten salt solutions are used.

Parabolic dish systems consist of a unit a parabolic dish reflector and its receiver at the focal point. The dish is tracked on two axes. Solar radiation collected by

receiver is absorbed by a gas which is used to operate a gas turbine. The turbines convert heat energy to mechanical energy that rotates the shaft of a generator.

Considering other solar thermal technologies such as the paraboloidal dish, central receivers, photovoltaic applications among others, parabolic trough power plants are the only type of solar thermal power plant technology with existing commercial operating systems (Price *et al*, 2010). In regard to commercially viable solar thermal power systems, a 354 MW solar energy generating station (SEGS) is established in California, U.S.A. where 134 GWh per year is generated (SWERA,2010), Nevada solar one is established on a 250 acre site in Nevada desert, where 50 MW of power are produced. Torressol and Arcosol are parabolic based plants that are established in Seville, Spain and produce 100 MW power annually. Others include a solar thermal power plant based on 1900 $m^2$of parabolic trough collectors that provide steam for a pharmaceutical plant (El Nasr project), Cairo, Africa. Andasol 1, 2 and 3 in Granada province, Spain produce 50 MW of power each annually. (Solar thermal power, 2010). In Egypt 40 MW of steam is generated by use of parabolic trough modules in Kuraymat. The steam is used as an input for a gas powered plant. A 25 MW parabolic trough power plant is constructed in Hassi R'mel in Algeria (Solar concentrators, 2011).

Tests conducted by scientists at the United States department of energy's National Renewable Energy Laboratory (NREL) showed that sky Fuel's parabolic trough meets high standards of efficiency (Arnold, 2010). This parabolic trough is located at solar energy generating station II in Daggett, California. It uses light weight reflec tech mirror film instead of glass mirrors. The steam produced achieves temperatures

above 350 ^{o}C and the concentrator's thermal efficiency of 73 %. Heat losses from the receiver were tested and optical efficiency of the concentrator measured. The optical efficiency is a direct gauge of the design elements in terms of mirror reflectance, parabolic curve accuracy, receiver alignment to focal line of trough and the systems tracking precision.

Andasol 1 in Gaudix, Spain uses parabolic trough solar concentrators consisting of long parallel rows of modular solar collectors. They use high precision reflector panels, which are checked photometrically to determine their alignment to the solar beam. Synthetic oil of car engines is used as the heat transfer fluid. It has an output capacity of 60 MW and generates steam at 400 ^{o}C (solar power, 2011).

Solar electric generating system (SEG 1) in Daggetti, California has an electrical capacity of 138 MW. It uses multilayered steel pipes as absorbers. They have an absorptance of 0.95 and emissivity of 0.14 at 400 ^{o}C (Parabolic solar steam, 2011).

1.3 Objectives

1.3.1 General objectives

To design, fabricate and characterize a prototype parabolic trough solar concentrator for steam production.

1.3.2 Specific objectives

1. To fabricate a prototype trough solar concentrator using appropriate materials.
2. To characterize collectors made with local materials i.e. aluminium sheet, car solar reflector and aluminium foil, and compare their efficiencies.

1.4 Problem statement

Global warming and environmental pollution are threatening existence of man on earth. They are caused by consistent use of fossil fuels and their products in large quantities. The carbon based fuels are the main sources of energy for majority of Kenya's population. Combustion of the said fuels leads to production of carbon dioxide which accumulates in atmosphere and causes global warming.

One of the ways to deal with the problems of global warming and environmental pollution is use of parabolic trough solar concentrators made of appropriate materials. Fabrication of such collectors would reduce the cost of power. Commercially available solar concentrators use high quality scarce reflecting systems to enhance performance. They also require technical expertise in their use, for instance evacuation of region surrounding the receiver, in design, characterization among other pertinent issues.

1.5 Justification

Amount of solar irradiation intercepted by earth and countries in the tropics e.g. Kenya, is high enough for harnessing. It is free of cost and predictable and without political influence and hence can be used to generate electrical power. Kenya, amongst other equatorial countries has a good percentage of their land with desert like conditions hence sparsely populated where modules of parabolic trough collectors can be placed.

Use of appropriate materials enhances design, fabrication and characterizations of PTSC's in that the materials used are locally available and require minimum surface

treatment i.e. scratch removal. The characterization adopted is affordable for the apparatus and equipments involved, locally available and well understood. The performance of the fabricated concentrators can be compared to performance of others by use of characterization.

1.6 Outline of the thesis

This thesis consists of five chapters. References and appendices are also included. Chapter one gives the introduction of the work done and related work that has been done in various parts of the world. It is also showing the objectives of the study, problem statement and justification. Chapter two gives the literature review of the main concepts that were used in design, fabrication and characterization of the three PTSC's and other related work done in other parts of the world. Chapter three gives the procedures and activities that were undertaken during design, fabrication and characterization of the solar concentrators. In chapter four data and information obtained in chapter three was analyzed and presented in a form that is easily understandable in establishing the performance of the fabricated concentrators. Conclusions and recommendations are found in chapter five. The references and appendices form the last part of this thesis.

CHAPTER TWO

LITERATURE REVIEW

2.1 Overview

Solar collectors transform short wavelength radiation of the range 0.29 μm - 2.5 μm into long wavelength and trap this energy in form of heat which is transferred to heat storage vault. Solar energy is harvested during sun hours. In the presence of the atmosphere, 1 kW/h per m^2 of sun energy is obtained from radiation energy (Ecoworld, 2000), Since one acre of land is equal to 4000 m^2 then 4000 kW/h of energy would be available per acre. Therefore solar heat energy has potential in industrialization but no major use has been recorded in Kenya due to lack of appropriate technology and expertise, so far the main application is cooking and space heating (SWERA, 2010).

It is necessary to achieve temperatures higher than 100 ^oC to generate steam power and therefore solar flux is concentrated onto an absorber. This is done by designing focusing or concentrating collectors such as the one shown in Figure 2.1.

The parabolic mirror focuses sunlight onto the focal axis where it is absorbed onto the surface of the absorber tube. The concentrator tracks the sun manually or automatically. For this concentrator, rotation about a single axis is adequate. High fluid temperatures can be achieved for direct steam generation.

2.2 Solar radiation geometry

In order to establish the beam energy falling on a surface of any orientation, the value of beam flux coming from the direction of the sun to is converted to an equivalent value corresponding to the normal direction to the surface. There are relations that make this conversion possible. Suppose θ is the angle between an incident beam of flux I_{bn} and the normal to a plane surface. Then the equivalent flux normal to the surface is given by $I_{bn}\cos\theta$. The angle θ is related through a general equation to latitude $\emptyset$, zenith angle θ_z, declination δ, surface azimuth angle φ , hour angle ω and+ slope β as given by Equation 2.1 (John *et al* , 1991).

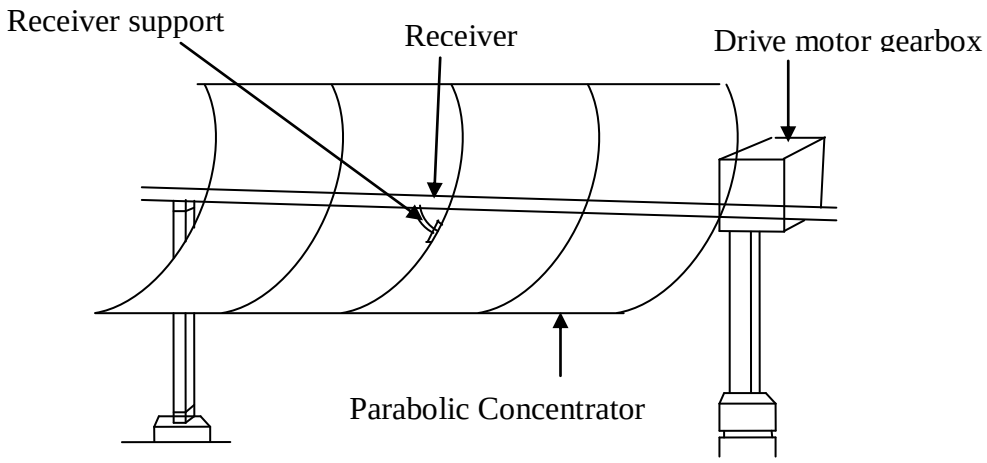

Figure 2.1: Cylindrical parabolic concentrating collector

$$\cos\theta = \sin\emptyset(\cos\delta\cos\beta + \cos\delta\cos\varphi\cos\omega\sin\beta) + \cos\emptyset(\cos\delta\cos\omega\cos\beta - \sin\delta\cos\varphi\sin\beta) + (\cos\delta\sin\varphi\sin\omega\sin\beta) \quad (2.1)$$

For a horizontal surface β = 0 and Equation 2.1 becomes:

$$\cos\theta = \sin\emptyset \sin\delta - \cos\emptyset \cos\delta \cos\omega \quad (2.2)$$

Figure 2.2 shows the relationship between these angles.

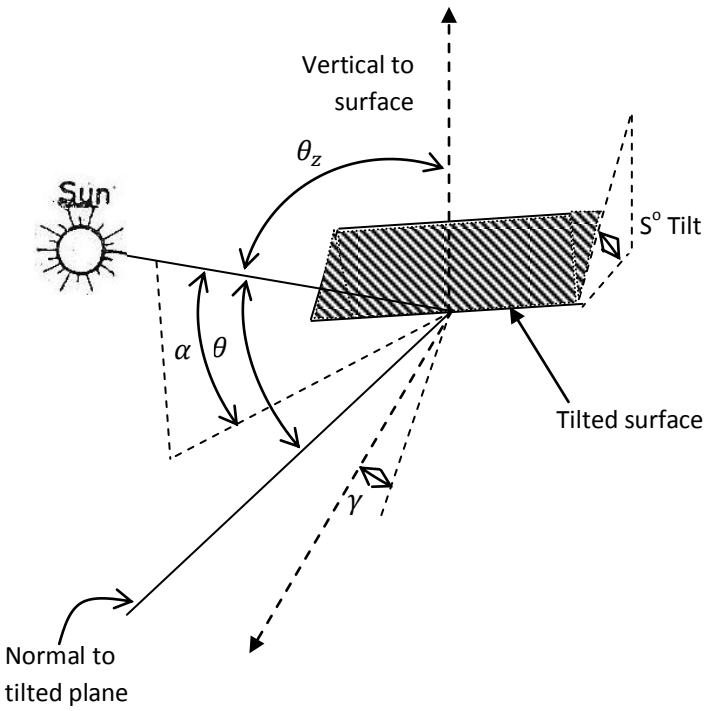

Figure 2.2: Relationship between various angles and the sun.

The hour angle corresponding to sunrise or sunset (ω_s) on a horizontal surface can be determined by Equation 2.3, (Twidel, 1986), for β = 0

$$\cos\theta = \sin\phi\sin\delta + \cos\phi\cos\delta\cos\omega \quad (2.3)$$

Substituting the value of 90° for zenith angle we obtain:-

$$\omega_s = \cos^{-1}(-\tan\phi\tan\delta) \quad (2.4)$$

From Equation 2.4, ω_s is positive in the morning and negative in the afternoon. 15^o of hour angle is equivalent to 1 hour. The time used for calculating the hour angle ω is the local apparent time. This is obtained from the standard time observed on a clock by applying two corrections. The first correction arises because of the difference between the longitude of a location and the meridian on which the standard time is based. It has a correction of 4 minutes for every degree difference in longitude. The second correction, called the equation of time, arises as a result of the earth's orbit and rate of rotation subject to small fluctuations.

2.3 Solar radiation on tilted PTSC surface

The ratio of beam radiation falling on a tilted surface to that falling on a horizontal surface r_b is shown in the equation below.

$$r_b = \frac{\cos\theta}{\cos\theta_z} = \frac{\sin\delta\sin(\phi-\beta)+\cos\delta\cos\omega\cos(\phi-\beta)}{\sin\phi\sin\delta+\cos\phi\cos\delta\cos\omega} \tag{2.5}$$

where:

$$\cos\theta = \sin\delta\sin(\emptyset-\beta)+\cos\delta\cos\omega\cos(\emptyset-\beta) \tag{2.6}$$

$$\cos\theta_z = \sin\emptyset\sin\delta+\cos\emptyset\cos\delta\cos\omega \tag{2.7}$$

The solar flux I_T falling on a tilted surface at any instant consists of both beam and diffuse radiations as shown in the following equation:-

$$I_T = I_b r_b + I_d r_d + (I_b - I_d) r_r \tag{2.8}$$

where

$I_b r_b$ is the beam radiation, $I_d r_d$ represents diffuse radiation and I_T represents total radiation on a surface:

The tilt factor for diffuse radiation is given by;

$$r_b = \frac{1+\cos\beta}{2} \tag{2.9}$$

The radiation shape r_r factor for a tilted surface with respect to the sky tilt factor for diffuse radiation is obtained using following equation:-

$$r_r = \rho\left(\frac{1-\cos\theta}{2}\right) \tag{2.10}$$

Ratio of the flux on a tilted surface, I_T at any instant to that on a horizontal surface, I_g is given by following equation:-

$$\frac{I_T}{I_g} = \left(1 - \frac{I_d}{I_g}\right) r_d + \frac{I_d}{I_g} r_d + r \tag{2.11}$$

The most important parts of a parabolic trough solar concentrator can be summarized as shown in Figure 2.3,

2.4: Parabolic trough collector geometry

A section of a linear parabolic concentrator showing major dimensions is as shown in Figure 2.4. The principal focus lies on an axis along the parabola. This is where the rays incident on the optical system are concentrated to heat the heat transfer fluid. Not all rays are brought to receiver by the optical system because some are lost at the edges and others are scattered by irregularities on the optical system. The principal focus may be projected out of the parabola if it is insulated against heat losses by covering it with an envelope of evacuated glass.

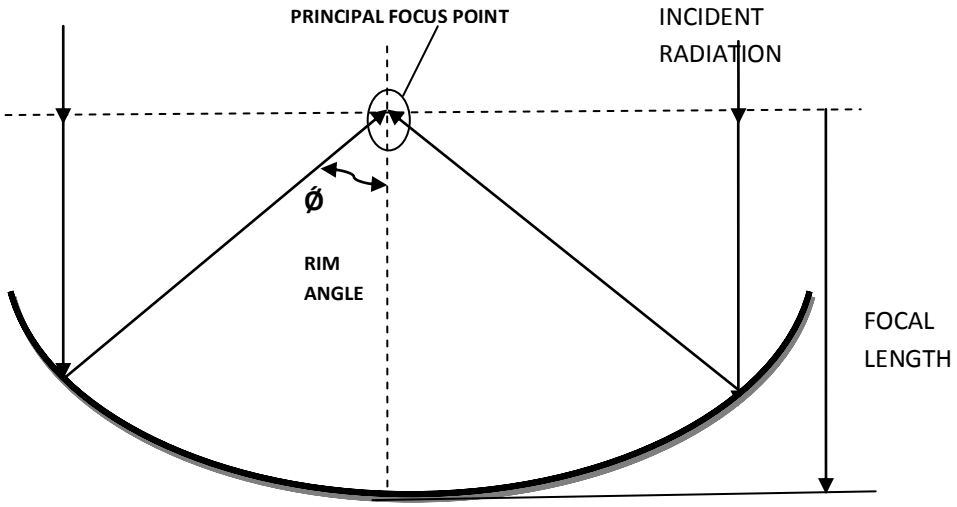

Figure 2.3: Basic geometry of a parabolic trough

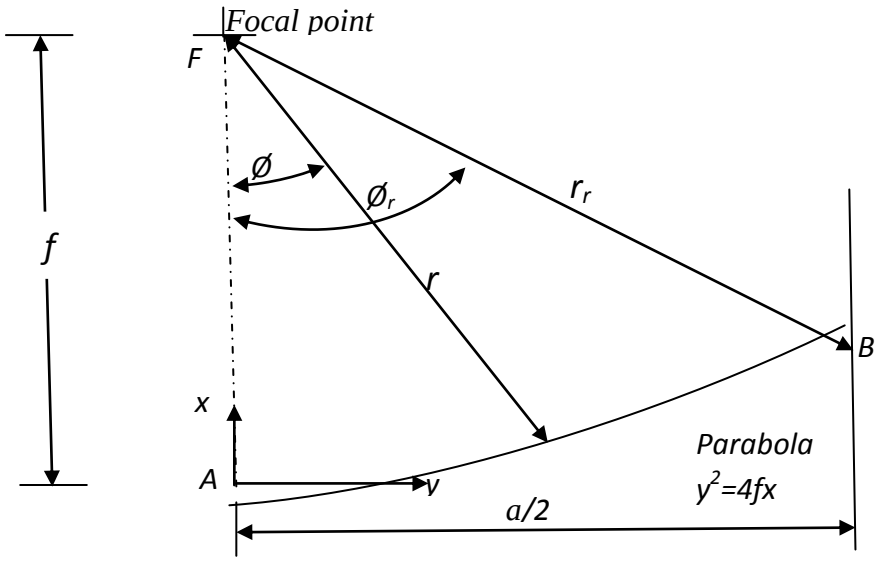

Figure 2.4: Main dimensions of a parabolic trough solar concentrator

In figure 2.4, *a*, is the aperture and *f* is the focal length. If a radiation beam from the sun's disk is incident on the reflector at point B on the rim where radius is maximum at r_r, the angle $ø_r$ is the rim angle given in the following Equation.

$$\emptyset_r = \tan^{-1} \frac{8\left(\frac{f}{a}\right)}{16\left(\frac{f}{a}\right)^2 - 1} \qquad (2.12)$$

An incident beam of solar radiation is a cone shown in Figure 2.5

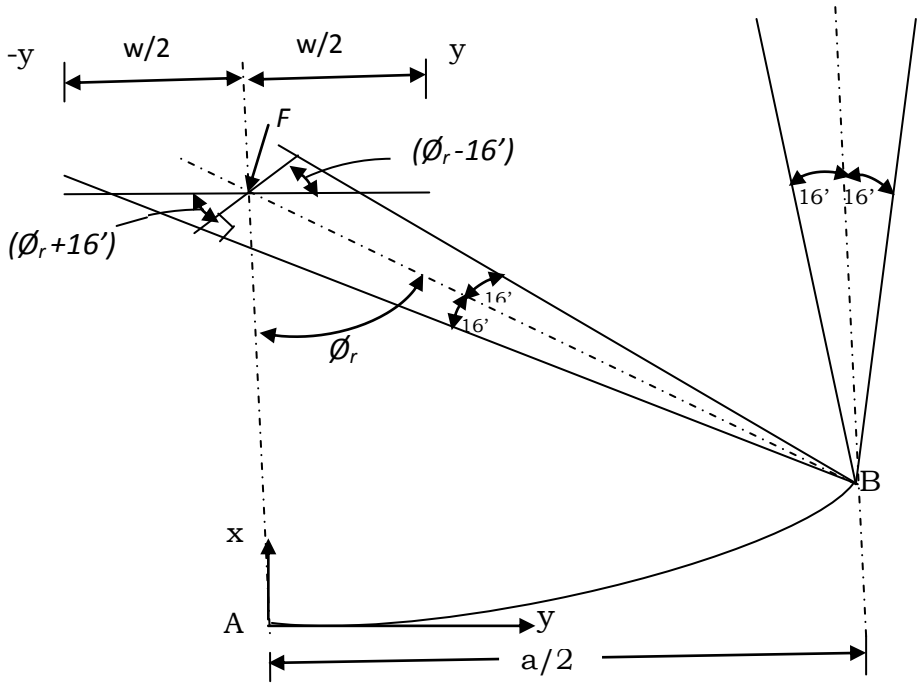

Figure 2.5: Reflection of a beam of the sun at collector angle

2.5 Parabolic trough collector testing

Standard testing and rating practice i.e. ASHRAE 93–77 (John, *et al)* provide an equitable basis for comparing efficiencies of different types of collectors and an essential basis for design and selections of equipment. Procedures to use as described here have been widely used and were initially proposed by the National Bureau of Standards (NBS) and the American Society of Heating Refrigerating and Air Conditioning Engineers (ASHRAE).

Efficiency, η_i is calculated from the following equation:-

$$\eta_i = \frac{q_u}{A_c I_T} = \frac{\dot{m} c_p (T_{2-} T_1)}{A_c I_T} \quad (2.13)$$

where q_u is the useful gain in heat, $\dot{m}$ is the mass flow rate, I_T is the beam radiation intensity, A_C is the collector area, c_p is the specific heat capacity of heat transfer fluid, T_2 is the outlet temperature of heat transfer fluid, T_1 is the inlet temperature of heat transfer fluid.

The data used is recorded under steady state conditions.

2.6 Parabolic trough solar concentrator and nomenclature

In this section design and some characteristics of fabrication materials are presented. One achievement by the parabolic trough concentrator is the 80 MW solar thermal electric power plants set up by Luz in California of the following dimensions and characteristics:- Aperture width: 5.76 m, length: 95.2 m, curved reflecting surface of glass mirror area: 224 m^2, reflectivity: 0.94, glass covers transmitivity: 0.965, outer absorber tube diameter: 0.003 m, tube surface absorptivity: 0.97, tube surface emissivity: 0.15, optical efficiency: 0.772, peak collection efficiency: 0.68 and annual collection efficiency:0.53 (Suhas, 1991).

The Euro trough model 150 had the following characteristics: Focal length; 1.71 m, absorber radius; 0.035 m, aperture width; 5.77 m, aperture area; 817.5 m^2, collector length: 148.5 m, number of glass facets: 336, mirror reflectivity: 0.94 and weight of steel structures, 18.5 kg.

Another Euro trough model collector consists of 12 m long collector modules. Nine commercial solar electric generating systems (SEGS), designed, constructed and

operated by Luz international operate in Mojave Desert of Southern California. (Solar Energy applications, 2010).

Three collector designs have been used in the plant described above. Reflectors are made of back silvered glass, low iron float glass panels which are shaped over parabolic forms. Metallic and lacquer protective coatings are applied to the back of the silvered surface and a measurable degradation of the reflective surface has been observed. The glass is mounted on truss structures, with the position of large arrays of modules adjusted by the hydraulic drive motors. Receivers are 0.07 m diameter steel tubes and 0.003 m in diameter with cermet selective surfaces surrounded by a vacuum glass jacket. The surfaces have an absorptance of 0.96 and emittance of 0.19 at 380 ^{o}C Reflectance of mirrors is 0.94 when clean and the total mirror area is 1.35 x 10^{6} m^{2}. Cleaning by machinery is done every two weeks. Synthetic heat transfer fluid is utilized (Renewable Energy, 2008).

The conditions of operation for these concentrators are such that the operating temperatures are higher, edge effects are more significant, conduction terms are quite high and radiation flux on receivers is also quite high compared to flat plate collectors (Renewable Energy, 2008). There may be no obvious general method of estimating thermal loses. However generalized analysis of a focusing collector system is very similar to that of flat plate collectors.

An energy balance equation provides heat gain per unit collector length *L*, as given in the following equation (John *et al*, 1991).

$$Q_u = \frac{A_a}{L} H_b r_b \rho \gamma (\alpha\tau)_b - \pi D_O U_l (T_m - T_a) \qquad (2.14)$$

D_o represents external diameter of absorber, A_a represents area of aperture, $H_b r_b$ represents solar flux intensity, ρ represents reflectance, α represents absorptance, τ represents transmittance, L represents *l*ength, U_l represents heat loss coefficient, T_m represents mean temperature of heat transfer fluid, and γ represents intercept factor.

The heat gain q_u can be obtained from Hottel – Whillier – Bliss equation, which is given by the following equation (Gillet, 1985).

$$q_u = \frac{A_a}{L} H_b r_b \rho \gamma (\alpha\tau)_b - \pi D_o U_l (T_m - T_a) \quad (2.15)$$

The collector efficiency factor, F' can be obtained from equation 2.16. It refers to the efficiency with which thermal heat is being absorbed, where, $H_b r_b$ is the solar beam intensity, A_a is the aperture area, L is the length of collector, S is the absorbed radiation, $(T_m - T_a)$ is the temperature difference, $(\alpha\tau)$ is the absorptance transmittance product, U_l is the heat loss coefficient, ρ is the reflectance and γ is the intercept factor.

The collector heat removal factor F_R is defined as the ratio of the actual heat gain of collector to the gain if collector surface were at inlet temperature of the heat transfer fluid which is obtained from the following equation (John, et al, 1991).

$$F_R = \frac{\dot{m} c_p (T_{fo} - T_{fi})}{\frac{A_a}{A_r} S - U_l (T_{fo} - T_{fi})} \quad (2.16)$$

where $\dot{m}$ is the mass flow rate of heat transfer fluid, c_p is the specific heat capacity of heat transfer fluid, F_R is the heat removal factor of collector, U_l the heat loss

coefficient, A_r is the receiver tube outer diameter, F' is collector efficiency factor, S is absorbed solar radiation energy.

So that total gain is obtained from the following equation,

$$Q_u = F_R A_a \left[\frac{A_r U_l}{A_a}(T_1 - T_a)\right] \tag{2.17}$$

Collector flow factor F'' is given by the following equation, (John et al, 1991).

$$F'' = \frac{F_R}{F'} = \frac{\dot{m}c_p}{A_r U_l F'}\left[1 - e^{\frac{F' A_r U_l}{\dot{m}c_p}}\right] \tag{2.18}$$

Collector efficiency is obtained from the following equation, (John et al, 1991).

$$\eta_c = \frac{Q_u}{H_b r_b A_a} \tag{2.19}$$

Optical efficiency η_{opt} is given by the following equation, (Rai, 1987).

$$\eta_{opt} = \rho\gamma\langle\alpha\tau\rangle \tag{2.20}$$

where ρ is the reflectance loss for the material under consideration. It can be determined experimentally. $\alpha\tau$ is the absorptance- transmittance product of the collector receiver and cover respectively and the γ is the intercept factor is the amount of the solar flux reaching the absorber. For parabolic trough system, the normal distribution curve for intercept factor can be expressed as shown in the following equation (Rai, 1987).

$$\frac{I}{I_{\max}} = e^{-h\left[\frac{\omega}{W}\right]^2} \tag{2.21}$$

The value of h is obtained from the following equation:-

$$I_{max} = \frac{1}{\sigma\sqrt{2\pi}} = \frac{h}{\omega\sqrt{\pi}} \tag{2.22}$$

where $I\ (\omega)$ is the radiation flux density that was received from the sun, I_{max} is the highest amount of flux reaching the absorber or the maximum flux density, ω is the distance from the centre of the zone of convergence of the solar flux accessing the absorber, W is the half – width (aperture) of concentrator, h is the normal flux distribution coefficient and σ represents the standard deviation of the normal distribution curve.

For parabolic trough concentrator which is being tracked, the distribution function is given by the following equation (Rai, 1987).

$$\frac{I}{I_{\max}} = e^{-h^2\left(\frac{r}{R}\right)^2} \tag{2.23}$$

and $$I_{\max} = \frac{1}{\sigma\sqrt{2\pi}} = \frac{h}{R\sqrt{\pi}}$$

where I is the radiative flux density at radial position from axis r/R, r is the radius in focal plane from axis and R is the concentrator rim radius

The intercept factor is obtained by use of the variables given by the following equation.

$$\gamma = \frac{I_{\max}\int_0^{\left(\frac{r}{R}\right)} e^{-h^2\left(\frac{r}{R}\right)^2} 2\pi\left(\frac{r}{R}\right)d\left(\frac{r}{R}\right)}{I_{\max}\int_0^{\infty} e^{-h^2\left(\frac{r}{R}\right)^2} 2\pi\left(\frac{r}{R}\right)d\left(\frac{r}{R}\right)} \tag{2.24}$$

Integration between the given limits in Equation 2.24 gives the following equation.

$$\gamma = 1 - e^{-h^2\left(\frac{r}{R}\right)^2} \tag{2.25}$$

CHAPTER THREE

MATERIALS AND METHODS

3.1 Introduction

In this section design and fabrication of three parabolic trough solar concentrators (PTSC) for steam production was carried out. Fabrication of some equipment needed for collector testing was also done e.g. fabrication of 6 Kw heater, heat exchanger and manual tracking system. Other parameters that were required in characterization were experimentally quantified to enhance the design of the PTSC s using appropriate materials.

3.2 Fabrication

3.2.1 Fabrication of concentrator

Angle iron metallic bars of dimensions 0.0015 m thick, 4 m in length and 2.4 m in width were curved into parabolic shapes with a focus at 0.04 m using the following equation.

$$y^2 = \frac{x}{4p} \tag{3.1}$$

Where x and y are Cartesian plane coordinates and p is the predetermined focal axis. Black sheets of dimension $4.8\ \text{m} \times 2.4\ \text{m} \times 0.001\ \text{m}$ were folded and welded onto angle iron beams on the outside. The edges of these sheets were folded to provide a rail which was lined with rubber sheets so that the glass covers slid smoothly as shown in Figure 3.1. The unequal thermal expansion between glass and metal would

not affect glass since the rubber sheets would be separating the two materials. The sides of the collector were closed with aluminum flashes.

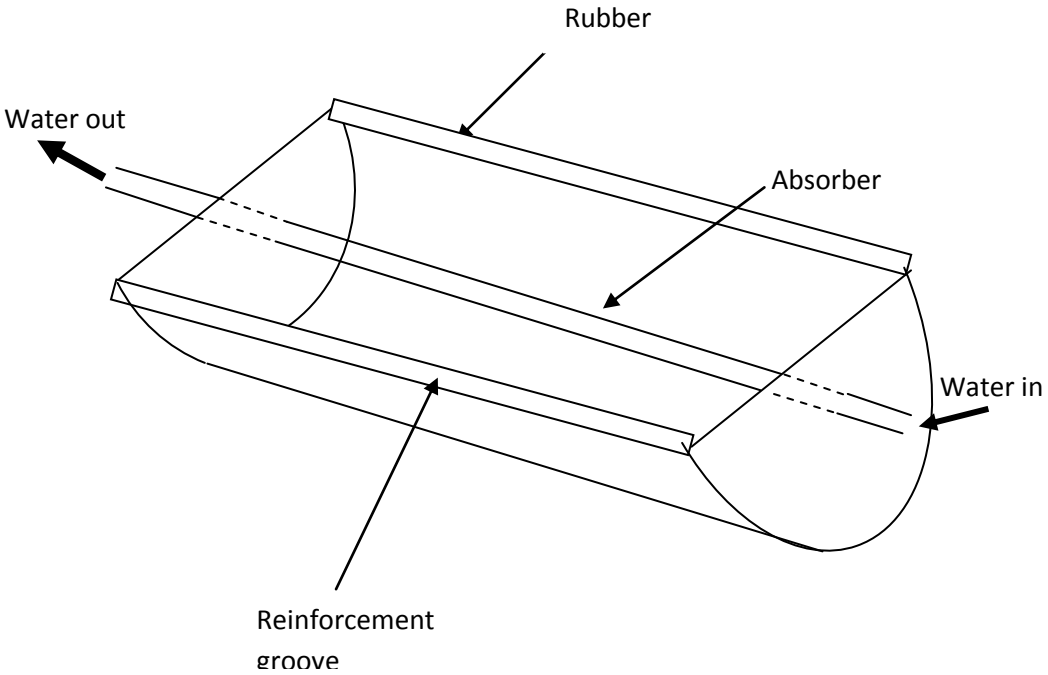

Figure 3.1*:* **General outlook of assembled solar collector**

The inner surface of the parabolic trough was laminated with the first reflector material known as aluminium sheet of dimensions 4.8 m × 2.4 m × 0.001 m of reflectivity , ρ as 0.8. The PTSC was of length 5.8 m and width 1.2 m as shown in plate A1. The glass covers were supported by small six box metallic bars of dimensions 0.022 m × 1.2 m. The receiver tube was suspended at principal axis using very thin mild steel wires. The parabolic trough concentrator was laminated with three appropriate materials each in turn i.e. aluminium sheet, car solar reflector and Aluminium foil (fay foil). The collectors were covered with glass that was 0.0025 m thick.

3.2.2 Fabrication of tracker

To fabricate the manual tracker, a winch was fabricated using general gears of 1:30 ratio and a class B black pipe of external diameter 0.008 m and internal diameter 0.007 m. The black pipe was fitted on one of the gear slots while on the other slot; a hook to effect the turning was fitted (Plate A2). The gears ensured that the parabolic collector could execute minute movements during tracking. A 0.05 m pin of diameter 0.003 m was placed at middle of collector aperture plane to track the sun. Various tracking pins were tested against the temperature obtained at the principal axis. The size that produced the best alignment of collector to the solar beam and hence registered highest temperature at focal axis was the 0.005 m pin in height and 0.003 m diameter. When the metallic pin cast a shadow, then the collector would be adjusted so that no shadow was cast and this would mean the solar beam from the sun disc was normal to the plane of collector. The collector was mounted to track the sun in the North –South orientation so that the solar image at absorber was less variable as the sun's position change during the day, compared to tracking in the East –West axis where the image of the sun on the receiver would be very much enlarged in the early and late hours of a day and of minimum size at noon.

3.2.3 Fabrication of heat exchanger

In order to cool the heat transfer fluid coming out of the collector, a heat exchanger was fabricated. This was done by fixing a coiled copper pipe of diameter 0.07 m inside a 100 liters plastic container. It was held fixed on to the inside of the container by back nuts and led to external connections by threaded unions. Thread tapes were used for the union connections. The container was then filled with cold

water that was frequently removed by siphoning it out and refilling to ensure effective cooling of heat transfer fluid coming out of the collector. This ensured that inlet temperature of the heat transfer fluid was well controlled during collector testing. Figure 3.2 shows the fabricated heat exchanger.

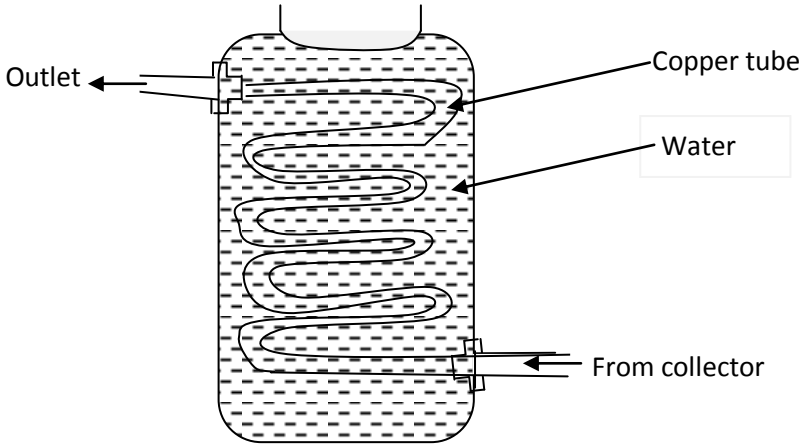

Figure 3.2: Fabricated heat exchanger

3.2.4 Fabrication of heater

To ensure that the testing temperatures changed from one to the next in a shorter time a 6 *k*W heater was fabricated. This was done by joining two, 3 kW, 240 *V,* heater elements which were soldered to a single base of one and the electrical terminals protruded. The earth terminal was the longest so that it also accommodated the cover nuts and bolts so as to close the cap and externally allow the asbestos insulated cables from heater terminals to proceed to the switch. The live terminal was connected to the thermostat which would be used to set the working fluid at a precise inlet, temperature, T_1. The thermostat used was of the range 50 – 300 ^{o}C and was adopted by putting the mercury tube into the middle slot

of thermostat for the heater. A 45 A water heater switch was used to control electricity flow to the heater. Figure 3.3 shows the fabricated heater.

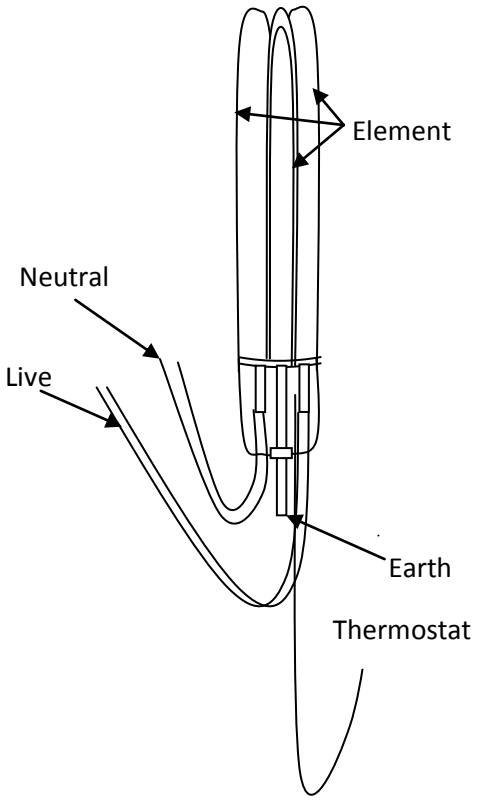

Figure 3.3: Fabricated heater

3.3 Measured PTSC parameters

In order to characterize fabricated PTSCs various measurements were taken. Use of these parameters provides means of designing solar collectors that are able absorb most of thermal energy from the sun. The rates of heat losses are reduced and because it is closed there is a time lag for it to cool

3.3.1 Measurement of concentration ratio

The concentration ratio parameters were obtained by measurements of aperture width, collector length and outermost diameter of absorber tube. The outermost area of absorber pipe was determined by calculating its circumference from measured diameter of the absorber tube as shown in Figure 3.4. The diameter was measured using electronic vernier calipers. Both inner and outer diameters were measured. The concentration ratio was calculated as shown in Section 4.2.

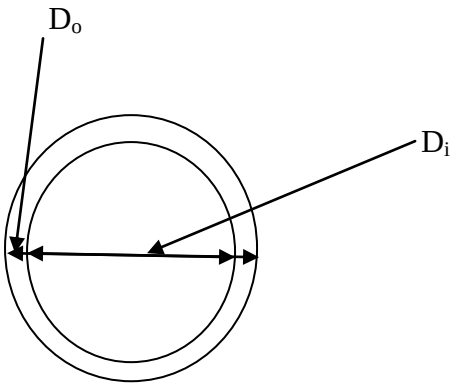

Figure 3.4: Diameters of absorber as measured by vernier calipers

3.3.2 Measurement of average heat absorbed by receiver

In order to measure the average heat that was absorbed by the receiver the following experiment was performed. The absorber used was made of copper tube of diameter 0.0025 m whose thermal conductivity was 3.9×10^2 J/Kg/K and Absorptance 0.9 (Hanssan, 1972). To determine the average heat that was absorbed by the receiver per unit time, it was partially filled with water. One end was closed using a control valve and the other end leading to a condenser was left open. The condenser was made of a plastic cylinder in which a coiled copper tube was fixed. The plastic

cylinder was then filled with cold water to condense the steam. The setup was operated until a steady state that was shown by water boiling in the receiver was achieved. The mass of steam condensed was measured using a beam balance and the time it took to obtain the steam was measured. The temperature at which steam was obtained was recorded. The following equation was used to find the average amount of heat absorbed, Q_{av} by receiver is given:

$$Q_{av} = \frac{mc\Delta\theta + mL_v}{t} \quad (3.2)$$

where m is mass of water, $\Delta\theta$ is change in temperature, L_v is the latent heat of vaporization of water, c is the specific heat capacity of water and t is time interval.

The rate of gain in heat $\dot{Q}$ is given by the following equation;

$$\dot{Q} = \frac{Q}{t} \quad (3.3)$$

where $\dot{Q}$ is the gain in heat, Q is the quantity of heat that is available and t is the time interval.

3.3.3 Measurement of solar irradiance

Measurement of solar irradiance was done using the calorimetric method. In this experiment a copper calorimeter of radius 0.03 m was insulated on the outside using aluminium foil and on the inside it was painted black. 0.05 g of water was poured in it and after settling a thermocouple probe was used to read initial temperatures of water. This calorimeter was left exposed at collector plane for 20 minutes and the

temperature read and recorded. Equation 3.4 was used to find solar beam irradiance I_b,

$$\alpha\tau A I_b = mc\frac{\Delta\theta}{\Delta t} \tag{3.4}$$

where:-

$\alpha\tau$ is beam transmittance – absorptance product, m is mass of water (kg) , density of water is 1000 kg/m^3, c is specific heat capacity of water, 4200 J/kg ^{o}C $\frac{\Delta\theta}{\Delta t}$ is the temperature change per unit time ^{o}C/s, A_a is aperture area and I_b is the beam irradiance. For a black body absorptance is unity. The material used for absorptance on the receiver pipe is treated as a black body.

The measurement of solar power intensity was measured throughout the day by recording the temperature changes of the water in the calorimeter every twenty minutes. The calorimeter was placed at the middle of the collector plane and secured with a thin cotton thread.

3.3.4 Measurement of intercept factor

The following experiment was performed in order to find the intercept factor for the fabricated concentrators. The fraction of the reflected radiation that was incident on the absorbing surface of receiver was measured by placing copper calorimeters with 0.025 kg of water at 4 equal distances from one another as shown in plate A4. Measurement of intercept factor was done before energy collection with each concentrator. Four calorimeters C_1, C_2, C_3 and C_4 were used in this experiment. These calorimeters were painted black on the inside and placed along the receiver

tube as shown in Figure 3.5. The copper calorimeters used in this experiment are represented by C_1, C_2, C_3 and C_4. The diameter and the depth of the calorimeters were 0.035 m and 0.065 m respectively. Temperature rise for the water in the calorimeter was measured. The time that was taken for the temperature of water to rise was also measured. Equation 3.4 was used to find the beam irradiance.

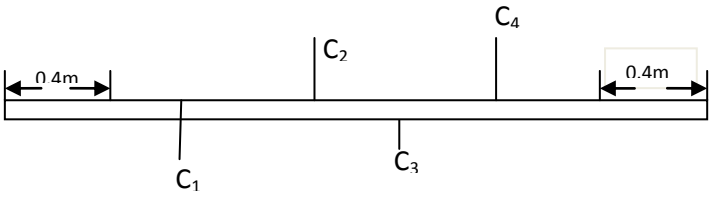

Figure 3.5: Arrangement of copper calorimeters on the absorber tube

The intercept factor distributions obtained from Figure 3.5 were averaged to obtain the intercept factor. The intercept factor, γ obtained from calorimetric method was determined using the equation below;

$$\gamma = \frac{Q}{A_s} \tag{3.5}$$

where Q is the heat absorbed by water in the calorimeter and A_s is the area of surface.

3.3.5 Measurement of heat loss rate and heat loss coefficient

The parameters that were used to find the heat loss rates and heat loss coefficient were measured in this section. These were: values of heat transfer fluids out let temperature, $T_{2:}$ heat transfers fluid's inlet temperature, T_1 and ambient temperature, T_a. These were measured over a period of time as the solar intensity declined, after every solar collection was done. The pressure drops across the collector were read from the pressure gauges. The values of mass flow rate were also measured.

Calculations and analysis of the heat loss rate and the heat loss coefficient were carried out as shown in Section 4.10.

3.3.6 Measurement of overall heat loss by absorber

The parameters that were measured in order to find overall heat loss coefficient for the absorber tube were observed in this section. The value of overall heat loss coefficient, U_l, was measured by heating the receiver electrically in laboratory. A constantan wire was inserted into sneak sleeve insulation and inserted into the receiver flow channel and the leads were properly insulated using asbestos insulated electric wires after which a plug was used to make the connection to the mains electricity. The potential drop across the terminals of the absorber tube was measured and the current that flowed was also measured. Time that was taken for the absorber tube to attain equilibrium temperature was measured. The values of potential drop across the absorber tube, current, time elapsed, equilibrium temperature of absorber and ambient temperature were obtained and shown in Section 4.3.

3.3.7 Optical performance measurements

Measurement of absorptance

In order to measure solar absorptance of the glass cover system used for the concentrators the following was done. The solar absorptance and transmittance of glass was measured by use of a photo spectrometer (Spectro-320) analyzer). The photo spectrometer was calibrated using a reference surface of Barium sulfate standards. The process involved calibration with a value of absorptance close to that of the materials to be tested. Figure 3.6 was used to obtain the absorption spectrum for the glass.

Measurement of reflectance

A spectrophotometer with an integrating sphere was used to find hemispherical reflectance of reflector materials that were used as reflecting systems in this work. These materials were aluminium sheet, car solar reflector and aluminium foil, for normal beam of incident radiation as a function of wavelength in the range from 200 - 800 nm.

Transmission /absorptance

In order to obtain the transmittance of the glass cover that was used in this work and also its absorptance the following setup was used. The transmittance spectra and absorptance spectra were obtained.

3.4 Treatment of absorber

The surface treatment of the receiver tube was carried out as described in this

section. The receiver tube was made of a cylindrical copper pipe of external diameter, D_o= 0.0025 m when painted with black board paint of emissivity, ε = 0.1 and solar absorptance of 0.9. The paint coat had to be kept thin so that there was minimum resistance to flow of heat through the coat and through mass of the pipe to the heat transfer fluid, which was water.

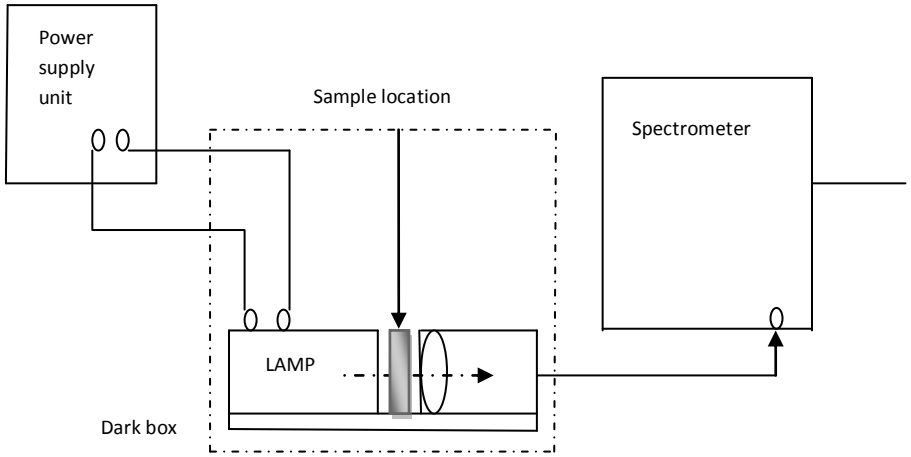

Figure 3.6: Set up that was used to determine transmission and absorptance.

The internal diameter of the absorber pipe D_i was 0.002 m and of effective length was 5.8 m .The collector was covered by use of glass cover whose transmitivity was 0.8. The cover reduced the rate of heat loss by conduction and convection, hence reducing the heat loss coefficient U_l

This reduction was as a result of suppression of convections heat loss by interposition of a relatively stagnant air layer between the inner section of the PTSC and glass cover, and by restriction of a long wave length thermal radiation in the collector chamber which was emitted back to the receiver.

3.5 Collector testing

3.5.1 Test installation

The collector test was carried out in Juja, latitude 1.1833 ° and 37.1167 ° in longitude. Collector mounting was done in a way not to obstruct the aperture of collector. An open mounting structure was made to allow free circulation of air as shown in Plate A2. Closed loop testing was used involving circulating pump, control valves and other components as shown in plate A2. Heat transfer fluid was water. The carbon black pipe was used to lead the heat transfer fluid into and out of collector. The G I (galvanized iron) pipe lead heat transfer fluid from the water bath to heat exchanger through to the pump since they are corrosion resistant. The pipe lengths between inlet and outlet of collector were kept as short as possible to reduce the effects of environment on fluid inlet temperature. The sections of pipe were lagged to minimize heat losses and were protected with reflective heat loss proof covers that extended beyond the temperature sensors to minimize heat loss or gain.

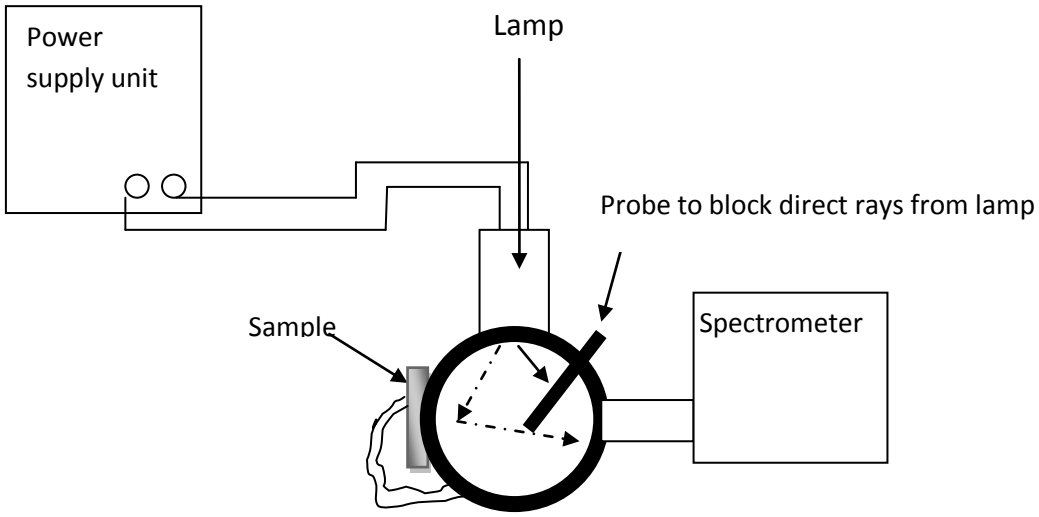

Figure 3.7: Setup used to determine reflectance.

The pipe bends (mixing devices) were introduced upstream after 0.2 m from the collector on its both ends. The pump was installed as shown in Plate A2 to ensure that the heat being lost by exiting fluid did not make attaining inlet temperatures difficult during collector testing. To this effect a bypass loop and a control valve were used to provide flow control. This also assisted in stabilizing the mass flow rate of heat transfer fluid.

3.5.2 Steady state

The length required for steady state test period was determined from thermal capacity *C* (fluid thermal capacity per square meter) of collector and the thermal flow rate mc_f of the heat transfer fluid through the collector. To ensure that a steady state was attained, the test period was made about four times the period defined by C/mc_f. Where c_f refers to specific heat capacity of heat transfer fluid. The time taken to attain steady state was found to be fifteen minutes. Collector fluid capacity was determined by filling the absorber with water which was then emptied into a measuring cylinder. The mass of the fluid it contained was measured to be 0.041 kg. The steady state period was determined as 15 minutes.

3.5.3 Temperature control

To control temperatures during the testing period, calibrated temperature sensors were used. Mercury in glass thermometer graduated at 0.05 ^{o}C intervals was used to calibrate the thermocouples which were used as temperature sensors. During installation good thermal contact between fluid and terminals of thermocouple was ensured by sinking their contacts deep inside the liquid flow channel through the

0.001 m holes that were drilled on the carbon black pipe connectors. In order to prevent overheating of the bath during the testing the heat transfer fluid was pre-cooled before being fed to thermostatic bath by use of a fabricated heat exchanger. The water in the thermostat bath was removed after every ten minutes by siphon and fresh cold water added to enhance its cooling effect.

3.5.4 Measurement of heat transfer fluid inlet temperature (T1) and exit temperatures (T2)

Plate A2 shows the thermocouples that were fixed at the inlet and outlet pipes of the concentrator under test. Temperature of heat transfer fluid at collector inlet and out let was measured to an accuracy of $\pm 0.1^{o}C$ surrounding air temperature was measured to an accuracy of $\pm$ 0.5 ^{o}C. The pressure tapping were installed normal to the flow. A hole of diameter 0.001 m on each side of mixing devices was made for the trappings. A smooth straight piece of pipe was incorporated before pressure tapping at inlet and outlet sections of the collector. Collector aperture area in reference was the transparent area of collector normal to incident solar flux. The heat transfer fluid flowed from bottom to the top of collector during testing. Before each day's testing period was carried out moisture was expelled from the concentrator by circulating heat transfer fluid at a temperature of approximately 90 ^{o}C until the moisture was removed. Collector pipe work was cleared of air trapped in heat transfer liquid by circulating the fluid at higher flow rate.

3.5.5 Collector test variables

Each of the fabricated concentrator was tested over their operating temperatures around solar noon. The tests produced data that was used in characterization. Data points for 4 fluid inlet temperatures spaced evenly over the operating range of the collector were used. The inlet temperatures of the heat transfer fluid that were used were: 90^{o} C, 140^{o} *C*, 190^{o} C and 240^{o} C. The test times were taken symmetrically about noon as follows: 11.00, 11.30, 12.30 and 1.00 p.m. This gave a total of 16 data points, taken before and after solar noon. The tests were made under steady state conditions. The test period for a steady state data point typically contained a time of approximately 15 minutes with correct fluid inlet temperature.

3.5.6 Collector testing loop

The collector testing was carried out at height of 3 m above the ground, on a building top. This was done to ensure economy of space usually utilized for agricultural activities. During the testing, the fabricated collectors were provided with heat transfer fluid at a precise inlet temperature, and the following measurements were also taken: pressure drop across the concentrator, mass flow rate and solar irradiance at the plane of the collector. These measurements were used in characterization where efficiencies, heat losses, heat loss coefficients and solar thermal steam pressures of different troughs were obtained compared. The testing used was carried out using the National Bureau of Standards (NBS) and the American Society of Heating, Refrigerating and Air Conditioning Engineers (ASHRAE) guide lines.

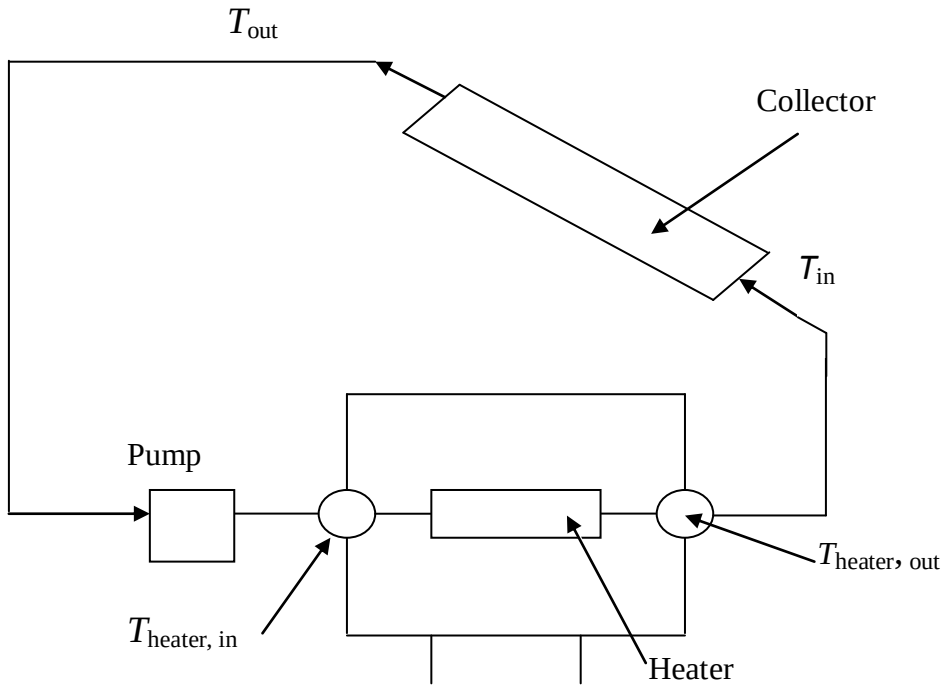

Figure 3.8: Collector testing set up

3.6 Production of steam

Each of the fabricated concentrators was used to harness solar thermal energy as shown in Figure 3.9. The water flow through absorber pipe was controlled by use of a control valve. A flow meter gave the mass flow rate of liquid turning into steam. Non return valves at the mixing joints prevented the back flow of steam when temperatures reduced. T_1 and T_2 are thermocouples measuring heat transfer fluid's Inlet and outlet temperatures respectively. The parabolic trough concentrators tracked the sun in a North-South orientation from the morning to the evening in this research; each for three days. The steam pressure values obtained were directly read from pressure gauges placed at inlet and out let mixing joints of heat transfer liquid. The values of temperatures of steam obtained were recorded along the pressure drop

values. The heat delivered by fabricated PTSCs was computed by use the following equation (Twidel, 1986).

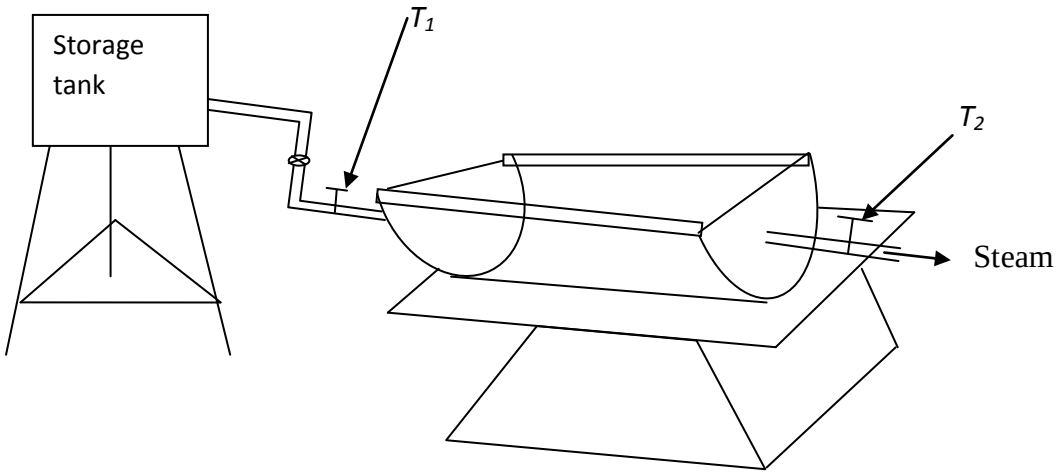

Figure 3.9: Setup for steam production

$$Q = \dot{m}\, c_p (T_2 - T_1) \tag{3.6}$$

where: $\dot{m}$ is the mass flow rate of heat transfer fluid, Q is the heat delivered by the receiver and $(T_2 - T_1)$ K is the temperature difference and c_p is the specific heat capacity of heat transfer liquid.

CHAPTER FOUR

RESULTS AND DISCUSSION

4.1 Introduction

In this section, results of designed and fabricated collectors and their characterization are presented in a form adequate for designing solar energy systems for roof tops. The focal point was chosen such that it was low so that the heat losses from the receiver pipe could be prevented by covering it with a glass cover; as a result the prototype parabolic trough solar concentrator had the focal axis in the inside. From Section 3.5 data was experimentally obtained to obtain collector efficiencies. Comparison of these efficiencies is also shown. Information is shown on how the fabricated concentrators absorb and lose energy; absorb solar thermal energy and the variations of solar steam pressure with temperature difference.

4.2 Determination of optical characteristics of reflecting systems

The Spectro-320 analyzer that was used had wavelength range of λ_1 = 200 nm to λ_2 = 800 nm. This was used to determine the absorptance and transmittance properties of the reflecting systems. Absorptance of the system can be computed from the following equation:-

$$\alpha_s = \frac{\int_{\lambda_1}^{\lambda_2} \alpha(\lambda) I_b \lambda \, d\lambda}{\int_{\lambda_1}^{\lambda_2} I_b \lambda \, d\lambda} \tag{4.1}$$

Where, α_s is the spectral absorptance, λ is wavelength and I_b is the solar beam intensity.

However in this work the spectrum obtained from the photo spectrometer was used to obtain the emittance of glass as 0.13. For opaque absorbers, absorptance may be obtained directly from the following equation:

$$\alpha(\lambda) = 1 - \rho(\lambda) \tag{4.2}$$

The spectral data that was obtained was considered against a blackbody spectrum for a reference temperature. In this work the reference temperature was taken as 473 *K*, which was the operating temperature of the collector

Measurement of reflectance

The reflectance of each of the reflecting materials i.e. aluminium sheet, car solar reflector and aluminium foil PTSC were measured for direct beam radiation.

The spectral distribution was wavelength dependent and the reflectance was integrated for spectral distribution of incident radiation. The specular reflectance ρ_s was defined as shown in the following equation, (Gillet, 1985).

$$\rho_s = \frac{\int_{\lambda_1}^{\lambda_2} \rho_{\lambda_s} I_{\lambda_j} d\lambda}{\int_{\lambda_1}^{\lambda_2} I_{\lambda_j} d} \tag{4.3}$$

Where I_{λ_s} represents specular reflected intensity of the solar flux incident on collector reflector, I_{λ_j} is the incident intensity of the solar beam.

The spectrum obtained for aluminium sheet was as shown in Figure 4.1

Tables I.1 and I.2 were used to give the energy increments for determination of reflectance for the appropriate materials that were used in this work. Ten equal increments of black body radiation were used from radiation tables. Table 4.1 shows

the reflectance that was obtained from the radiation tables, by considering them against ten increments that were obtained from the spectrum in Figure 4.1.

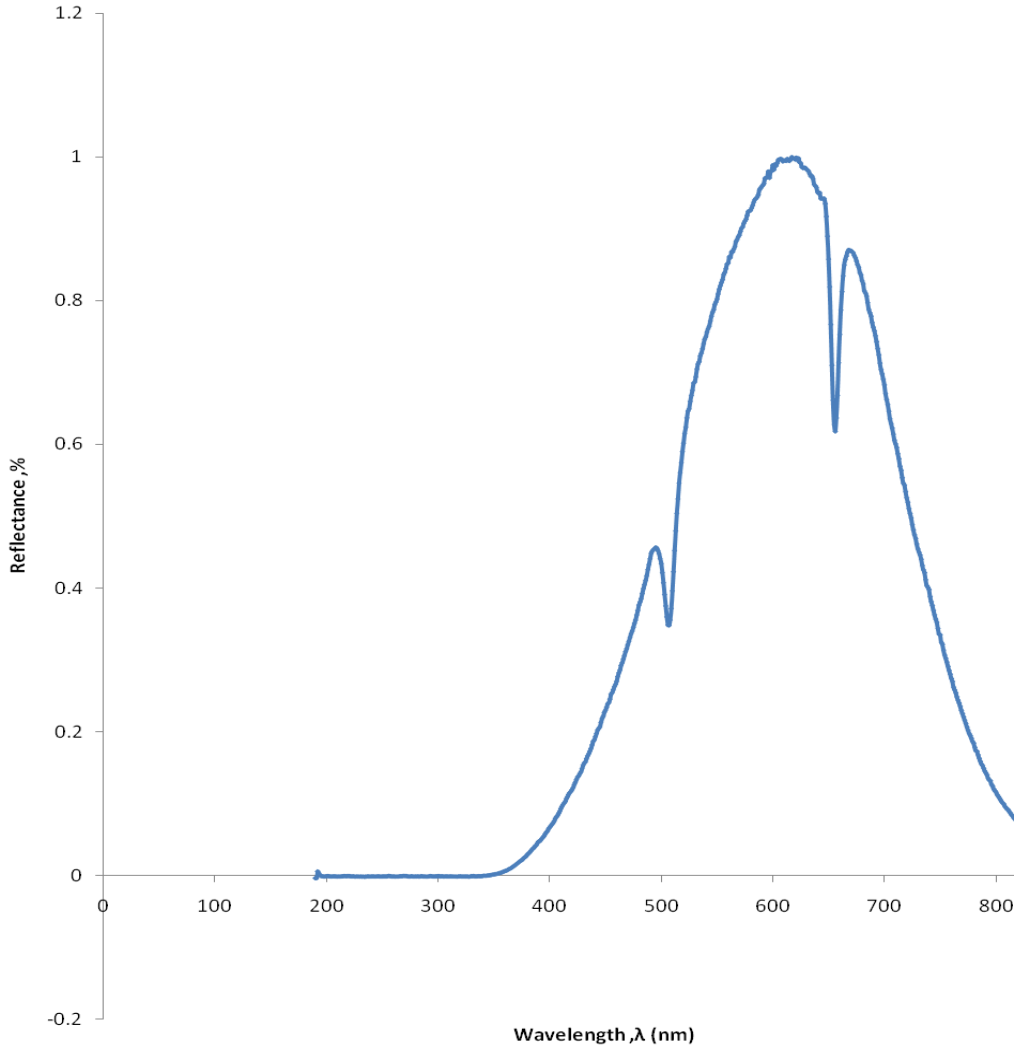

Figure 4.1: Aluminium sheet spectrum

The fraction of black body radiation energy between zero and λT and for even fraction increments is shown by Table 4.1 that gives the midpoint radiation energy that is used to calculate the midpoint wavelength. The value of the wavelength corresponds to wavelength on the experimental spectrum. For each increment indicated as, $\lambda_j T$, midpoint wavelength at temperature of reference was found from

the Table 4.1. Midpoint wavelength, λ_j for each increment was calculated from $\lambda_j T/T$ and reflectance was determined from the spectrum obtained from spectro – 320 analyzer.

Table 4. 1: Table of increments used

Increments $\Delta f_{j,}J$	$\lambda_j T_{mid}$ µmK	λ_{jmid}, µm	ρ_{λ_j}
0.0-0.2	2200	4.65	0.83
0.2-0.4	3120	6.60	0.75
0.4-0.6	4110	15.05	1.0
0.6-0.8	5590	11.82	0.8
0.8-1.0	9380	19.83	0.8

The first increment had wavelength range of 0 – 2680 µmK. The average temperature considered for operation was 473 K, so that the wavelength for the first increment was obtained as 5.7 µm.

The midpoint $\lambda_j T$ was 2200 µmK and λ_j was obtained as 4.65 µm and the reflectance for this spectrum was obtained from Table 4.1, as 0.83. All the increments used were equal and reflectance of aluminium sheet was obtained as 0.83. Emissivity was obtained using the following equation as 0.17

$$\varepsilon = 1 - \frac{1}{n} \sum_j^n \rho_{\lambda_j} \quad (4.4)$$

Determination of absorptance of glass was carried out as follows: Ten equal increments of energy (terrestrial) radiation were considered against ten equal

increments obtained from the fabricated PTSC collectors' absorptance spectrum. The ten equal energy increments that were used were obtained from Table H.1

For the increments that were considered in Table H.1, the midpoint wavelengths λ_{mid}, μm were obtained and the average reflectance was found from the reflectance spectrum of the material. Table 4.2 gives reflectance for the energy increments.

Table 4.2: Reflectance of aluminium sheet spectrum

Increment Δf_j	λ_{mid},μm	ρ_λ
0.0-0.1	0.434	0.04
0.1-0.2	0.517	0.06
0.2-0.3	0.595	0.07
0.3-0.4	0.670	0.08
0.4-0.5	0.752	0.09
0.5-0.6	0.845	0.10
0.6-0.7	0.975	0.14
0.7-0.8	1.01	0.55

Absorptance was obtained as α = 0.36, from the following equation.

$$\alpha = 1 - \frac{1}{n}\sum_j^n \rho_{\lambda_{ij}} \quad (4.5)$$

The absorptance of a 0.003 m single glass cover is 0.3 (Rai, 1987).

The reflectances of aluminium sheet, car solar reflector and aluminium foil concentrators are shown in Table 4.3 and also compared with those of documented

collectors. Optical efficiencies of the systems were determined in a similar manner as shown above on aluminium sheet and presented in Table 4.4.

Table 4.3: Reflectance for fabricated PTSC and documented PTSC

PTSC	REFLECTANCE
FABRICATED PTSC	
Aluminium sheet	0.83
Car solar reflector	0.81
Aluminium foil	0.78
DOCUMENTED PTSC(Solar energy applications, 2010)	
Luz collector	0.94
Euro Trough	0.94

The transmitivity of the glass cover used was 0.78 as obtained from the transmittance experimental spectrum while the cover transmittance for Luz collector was 0.965 and for Euro Trough was 0.95 (John *et al*, 1991). Emissivity of glass used in this work was obtained from experimental values and found to be 0.36 and absorptance was found to be 0.25. The glass used was 0.0025 m thick. The absorptance of 0.003 m low iron glass is 0.17 (Solar thermal resource, 1999).

Table 4.4: Optical efficiency for the fabricated concentrators

PTSC	OPTICAL EFFICIENCY
Aluminium sheet	0.53
Car solar reflector	0.56
Aluminium foil	0.47

4.3 Overall heat loss coefficient, U_l

To find the overall heat loss coefficient for the absorber, following data was obtained from section 3.3.6: *V* as 240 V, *I* as 2 A, *t* as 88.18 s, equilibrium absorber temperature, T_{abs} as 41.5 K and ambient temperature, T_a as 21.4 K. The following equation was used to obtain overall heat loss coefficient as 304.5 W/m^2. (Rabl, 1985)

$$U_l = \frac{\dot{Q}_{elec}}{A_a\,(T_{abs} - T_a)} \tag{4.6}$$

where, $\dot{Q}_{elec}$ is rate of electric power use, A_a is effective aperture area, T_{abs} is equilibrium absorber temperature, T_a is ambient temperature and U_l is Overall heat loss coefficient.

4.4 Average heat absorbed by receiver, Q_{av}

The receiver absorbs solar thermal energy from the sun and transmits it to the heat transfer fluid. The average amount of heat that was absorbed by the receiver was obtained as 886.93 W/m^2 by use of Equation 3.2. Using the insolation that was

obtained from Section 4.5, as 852.7 W/m^2, the amount of power that can be harnessed from an area covered with collectors can be obtained as follows: For the fabricated collectors of aperture area 6.95 m^2, the power that can be collected in one hour neglecting external losses as described in section 3.6 would be 3.19×10^6 W. If an array of collectors was used to cover one acre, the power that would be collected would be 9.27×10^6 MW from steam at an average temperature of 150 ^{o}.

4.5 Determination of solar irradiance

The heat gain was calculated from the following equation (Twidel *et al,* 1986).

$$Q = mc_p \frac{\Delta\theta}{\Delta t} \tag{4.7}$$

Rate of heat gain was calculated as 2.4 J/s from Equation 3.3. Area of circular calorimeter base A_b was obtained as 2.82×10^{-3} m^2. Solar power per m^2 was obtained as 852.7 W/m^2 from variables measured in Section 3.3.3 by use of equation 3.2. This value is in close agreement with 849.5W/m^2 (Kariuki, 2006).

4.6 Determination of concentration ratio

The concentration ratio, *CR* was determined as 128 from the following equation

$$CR = \frac{A_a}{2\pi rl} \tag{4.8}$$

The circular absorber tube area, A_r was obtained from $A_r = \pi dl$. Where d represents the outer diameter of the absorber tube and l represents length of the absorber tube. Rim angle ϕ_r was obtained as 74.87 ^{o} from the following equation.

$$\phi_r = \tan^{-1}\left[\frac{8\left(\frac{f}{a}\right)}{16\left(\frac{f}{a}\right)^2 - 1}\right] \quad (4.9)$$

where *f* is focal length of PTSC and *a* is the aperture of PTSC.

Optical properties of the concentrator were used to obtain absorbed radiation, *S*, per unit area of exposed aperture for each of the concentrators. For aluminium sheet, the absorbed solar radiation was obtained as 466.2 W/m^2 by use of the following equation.

$$S = I_b \rho \gamma \langle \alpha\tau \rangle \quad (4.10)$$

where, S is absorbed solar radiation; I_b is the solar beam radiation normal to collector aperture, as 852.7 W/m^2 ; ρ is the reflectance of aluminium sheet as 0.8, ; γ is the intercept factor as 0.76 and $\langle \alpha\tau \rangle$ is the absorptance- transmittance product as 0.9. The absorbed solar radiation by Car solar reflector PTSC and Aluminium foil PTSC were obtained in a similar manner using the Equation 4.10 as 449.5 W/m^2 and 397.2 W/m^2 respectively.

4.7 Intercept factor determination

Plate A4 shows the experimental set up that was used to measure intercept factor of the solar collectors fabricated in this work. The intercept factor determination at noon was carried out as described in 3.3.4 from the following data: - cylindrical surface area of the calorimeter was 0.010995 m^2 and surface area of cylindrical

absorber superimposed by calorimeter was 5.498×10^{-4} m^2. Surface area ratio of the two areas was 1: 19. Solar thermal energy absorbed by water in calorimeter was obtained as 1.299×10^3 W/m^2 using Equation 3.3. Intercept factor was obtained as 649.84 W/m^2. The values of calorimetric intercept factor results for aluminium sheet collector were: 649.84 W/m^2, 591 W/m^2, 658.7W/m^2 and 633.1 W/m^2 for the four calorimeters shown in plate A4. These were obtained from Equation 3.4. These values were averaged and the intercept factor obtained was 627.8 W/m^2.

4.8 Fabricated collector characterization

4.8.1 Efficiency characterization for closed fabricated collectors

In this section the fabricated solar collectors were characterized in terms of efficiency for both closed and open solar collectors, heat loss rate and heat loss coefficient, solar thermal energy collection and in terms solar thermal pressure output. This characterization is used in design of solar collectors so that the efficiency, solar thermal energy and steam pressures for a collector are enhanced and heat losses are minimized. In order to carry out efficiency characterization the following equation was used

$$Q_{u=} \frac{A_a}{A_c} F_R[I_b \rho \gamma \langle \alpha\tau \rangle - U_l (T_m - T_a)] \quad (4.11)$$

and

$$\eta_i = \frac{Q_u}{A_a I_b} \quad (4.12)$$

Where Q_u is the useful gain in heat by collector, η_i is the efficiency, A_a is aperture area, A_c is the collector area, F_R is the collector heat removal factor, I_b beam irradiance, ρ is reflectance, γ is the intercept factor, $\alpha\tau$ is the absorptance

transmittance product, U_l is the overall heat loss coefficient, T_m is mean temperature of heat transfer fluid and T_a is the ambient temperature.

Material 1: Aluminium sheet

In order to characterize the three fabricated PTSC for steam production, efficiencies obtained from equation 2.12 were plotted against $(T_m - T_a)/I_b$ Km^2/W. Where T_m is average temperature of heat transfer fluid, T_a is ambient temperature and I_b is solar beam normal to the concentrator aperture. To obtain the x-axis variable, the temperature difference between values for average inlet and outlet temperatures and ambient temperature as a ratio of normal beam solar irradiance were evaluated.

The efficiency figures show the principle design parameters that affect concentrator performance heat losses (slope with negative gradient) and absorption of solar radiation seen in optical efficiency being highest for ratio of temperature difference of zero and constant beam intensity.

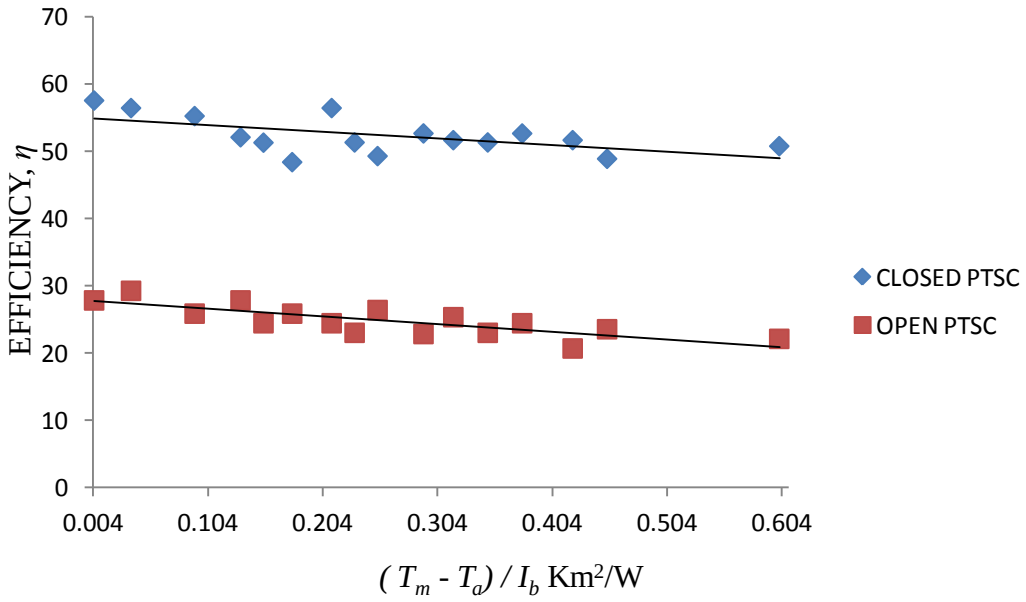

Figure 4.2: Characterization efficiency graph for aluminium sheet PTSC

Efficiencies obtained from Equation 2.12 were plotted against $(T_m - T_a)/I_b$ Km^2/W. Where T_m was the average temperature for the fluid outlet temperature and inlet temperatures. The increase in the ratio of temperature difference and a constant solar beam showed that increase in temperature difference of heat transfer fluid for a constant normal beam irradiance led to significant heat losses hence reduced efficiency. Efficiency varied linearly with $(T_m - T_a)/I_b$ Km^2/W and decreased as $(T_m - T_a)/I_b$ Km^2/W increased. It is seen that efficiency reduced with increase in heat transfer's temperature difference and an increase in operational temperatures of the concentrator caused more heat loses as seen from Figure 4.2. Most useful energy gain is available for collection when solar power intensity is high. It was assumed that $U_l F_R$ and $\propto \tau$ in the following equations are constants.

$$\eta_{opt} = F_R \rho \gamma \langle \alpha \tau \rangle \left(\frac{A_a}{A_c} \right) \tag{4.13}$$

$$U_l = F_R U_l \left(\frac{A_a}{A_c} \right)$$

(4.14)

Where η_{opt} and U_l are optical efficiency and overall heat loss coefficient respectively. The value of Equations 4.12 and 4.13 was obtained from efficiency graphs. U_l (overall heat loss) was found to be a weak function of temperature and corresponded to F_R as seen in energy balance Equation 2.17. The scatter in the data results is from variations in proportions of beam proportion of solar radiation, temperature dependency, wind effects, variations in angle of incidence etc. The value of efficiency is based on effective aperture area, A_a.

For this analysis average T_a = 21.8 K, T_m = 152.2 K, I_b = 752 W/m^2, ΔP = 921000 Pa and $\dot{m} = 8.8$ kg/s. where T_a is the ambient temperature, T_m is the average heat transfer fluid temperature and I_b beam radiation normal to the plane of collector. For open aluminium sheet solar collector: $\dot{m} = 3.98$ kg/s, $I_b = 749.3$ W/m^{2}and ΔP = 372000 Pa. The value of collector of efficiency was obtained using aperture area. Efficiency of closed fabricated concentrator was obtained from experimental variables and the following equation obtained as 54.65 %. The efficiency is determined as the ratio of heat energy output of the collector and the solar energy input from the incident solar energy as shown in the following equation. Useful heat gain was obtained from Equation 4.11 as 3230.72 J. Where Q_u is the useful gain in heat in hourly basis, A_a is the aperture area, F_R is the collector heat removal factor, I_b is the solar beam irradiance at the plane of the collector, ρ is the reflectance, γ is the intercept factor, α is the absorptance, τ is the transmittance, U_l is the overall heat loss coefficient and $(T_m - T_a)$ is the temperature difference, T_m is the average temperature of heat transfer fluid. The heat loss coefficient for aluminium sheet collector was obtained as - 3.92 W/m^2 from Figure 4.2.

Other fabricated concentrator characteristics

Absorptance- transmittance product refers to the ratio of flux absorbed in the receiver to the one incident on cover system, $\alpha\tau$. The transmittance absorptance product was obtained by use of the equation below as 0.8. The absorptance of copper was read from a reference hand book (Hanssan, 1972) as 0.9.

$$\langle \alpha\tau \rangle = \frac{\alpha\tau}{1-(1-\alpha_g)\rho_d} \tag{4.15}$$

where ρ_d represents the reflectance of cover system for diffuse radiation incident from bottom side.

where ρ_d = 0.15, α_g is absorptance, which is 0.3 for single glass cover, τ is transmittance of cover, α = 0.9 which is absorptance of receiver (Rai, 1987).

Emissivity of the glass cover system was obtained as 0.17 from the spectral distribution. Collector heat removal factor F_R was obtained from experimental data as 0.9 using the following equation (John et al, 1991).

$$F_R = \frac{\dot{m}c_p}{A_r U_l} \left[1 - e^{-\frac{F' A_r A_a}{\dot{m}cp}}\right] \quad (4.16)$$

Table E.1 shows the collector heat removal factors that were obtained for the fabricated collectors. Collector efficiency factor F' was also obtained from Equation 4.17 as 0.6. Table E.2 shows the collector efficiency factors that were obtained for the fabricated collectors. The equation below was used to find the collector efficiency factor.

$$q_u = F' \frac{A_a}{L} \left[S - \frac{A_r}{A_a} U_l (T_m - T_a)\right] \quad (4.17)$$

Collector flow factor, F'' was obtained from Equation 4.18 as 1.5 for aluminium sheet collector. Table E.2 shows the collector flow factors that were obtained for the fabricated collectors obtained in a similar manner.

$$F'' = \frac{F_R}{F'} \quad (4.18)$$

Optical efficiency, η_{opt} for aluminium sheet was obtained as 0.529 by use of the following equation (Kaligorou, 1991).

$$\eta_{opt} = \rho\gamma\langle\alpha\tau\rangle \quad (4.19)$$

Material II: Car solar reflector

The efficiency shown in Figure 4.3 was obtained by use of Equation 4.12. The values of q_u, A_a and I_b were obtained by experiment.

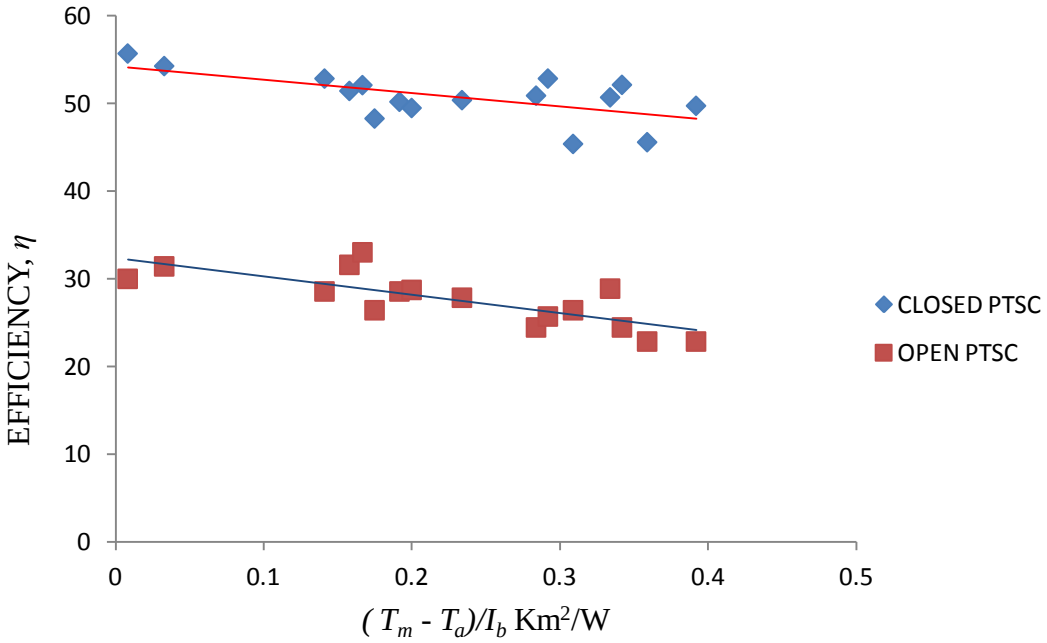

Figure 4.3: Characterization graph for car solar reflector PTSC

The average parameters used in this analysis were; T_m = 210 K, T_a = 22.7 K. For the closed collector $\dot{m}$ = 8.0 kg/s, I_b = 752.1 W/m^2 and ΔP = 870000 Pa. For the open car solar collector: $\dot{m}$ = 4.78 kg/s, I_b = 749.3 W/m^2 and ΔP = 397000 Pa

The value of efficiency was obtained from Figure 4.3 as 53.16 %. Useful heat gain was obtained from Equation 4.11 as 3147 W/ m^2.

Other fabricated concentrator characteristics

The transmittance- absorptance product was obtained from Equation 4.15 as 0.8. Collector heat removal factor F_R was obtained from Equation 4.16, as 0.87. The collector flow factor for car solar reflector PTSC was obtained from Equation 4.18 as 1.5. The heat loss coefficient for this material was obtained as – 408.30 W/m^2 from Figure 4.3. Optical efficiency was obtained from Equation 4.19 as 0.56.

Material III: Aluminium foil (fay foil)

In this analysis the average experimental parameters that were used were; T_m = 198 K, T_a = 22.5 K. For closed concentrator $\dot{m}$ = 7.8 kg/s, I_b = 837.4 W/m^2 and ΔP = 745000 Pa. For the open concentrator $\dot{m}$ = 4.08 kg/s, I_b = 850 W/m^2 and ΔP = 411000 Pa. Efficiency was obtained as 49.26 % from Figure 4.4. The useful heat gain was obtained as 2916 W from Equation 4.11.

Other fabricated concentrator characteristics for aluminium foil PTSC.

The absorptance transmittance product, $< \tau\alpha >$ was obtained from Equation 4.15 as 0.78. This was because of the thermal cycling of the glass cover and the absorber, which caused it to get lowered. Collector heat removal factor F_R was obtained from Equation 4.16 as 0.85. The collector efficiency factor was obtained from Equation 4.17 as 0.56. Collector flow factor F'' is obtained from Equation 4.18 as 1.52. From Figure 4.4 the heat loss coefficient obtained was - 26.12 W/m^2. The efficiency obtained for open aluminium sheet PTSC was 48.20 % from Figure 4.2 and its overall heat loss coefficient was obtained as -48.20 W/m^2 from the same figure. The closed solar concentrators gave higher performance efficiencies compared to the open ones. This was because the glass cover on closed solar collectors reduced heat

losses by convection and some radiation absorbed by the glass cover raised its temperature hence reducing the rate of upward transmission of heat from receiver. This reduction in the losses showed an effect of increasing transmittance absorptance product as seen in Figures 4.2, 4.3 and 4.4.

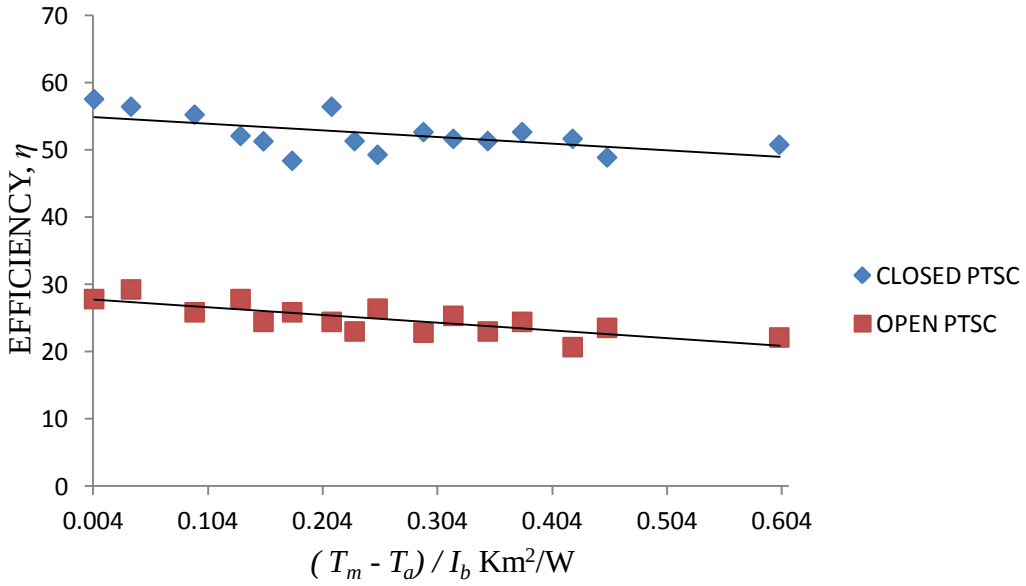

Figure 4.4: Characterization efficiency graph for aluminium foil PTSC

4.9 Heat loss

4.9.1 Heat loss characterization

Heat lost by a concentrator lowered its thermal efficiency. The higher the rate of heat lost by the concentrator the lower its output would be. In design of solar concentrators the heat loss rate is kept at a minimum.

Material I: Aluminium sheet

Heat loss and heat loss coefficient for aluminium sheet

The overall heat loss rate for parabolic trough concentrator was obtained from the following equation, (Gillet, 1985) and plotted against temperature difference.

$$\dot{Q} = \dot{m}\, c_p (T_1 - T_2) \tag{4.20}$$

T_1 - fluid inlet temperature. T_2 - fluid outlet temperature.

Overall heat loss coefficient was obtained from the following equation, (Gillet, 1985) and was plotted against temperature difference.

$$U_l = \left(\frac{\dot{m}}{A_a(T_2 - T_1)}\right) \tag{4.21}$$

The heat loss rate of the fabricated sheet solar concentrator was observed to increase in increase in the solar thermal energy collected by the concentrator. To reduce the heat losses insulation was done by covering the exposed parts of the receiver pipe with aluminium foil. This was repeated for all the fabricated concentrators. It was also observed that an appropriate material which had the highest number of creases as a result of handling produced the lowest overall efficiency. The appropriate materials underwent thermal degradation under high operational temperatures.

Material I: Aluminium sheet

Figure 4.5 shows the heat loss rate by aluminium sheet PTSC and Figure 4.6 shows heat loss coefficient as a function of temperature difference for the same collector.

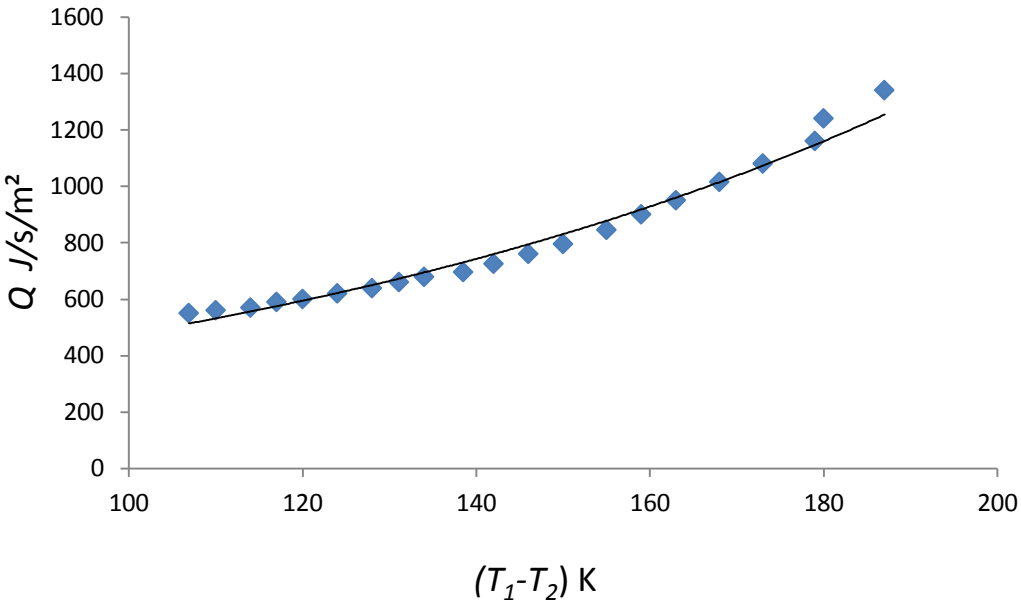

Figure 4.5: Heat loss rate for aluminium sheet PTSC

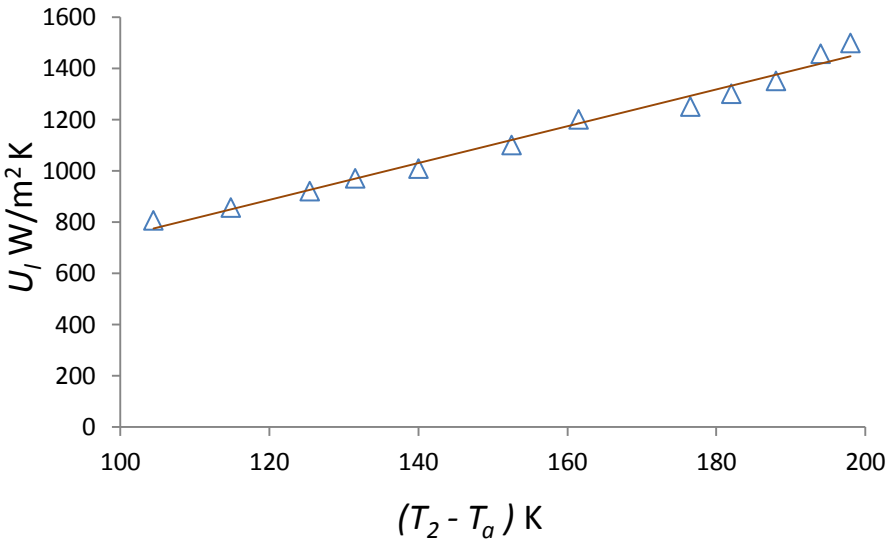

Figure 4.6: Overall heat loss coefficient for aluminum sheet PTSC

Material II: Car solar reflector

The following analysis shows how car solar PTSC lost heat to the surroundings.

Heat loss rate and heat loss coefficient

Figure 4.7 shows heat loss rate by car solar reflector PTSC and Figure 4.8 shows heat loss coefficient as a function of temperature difference for same collector.

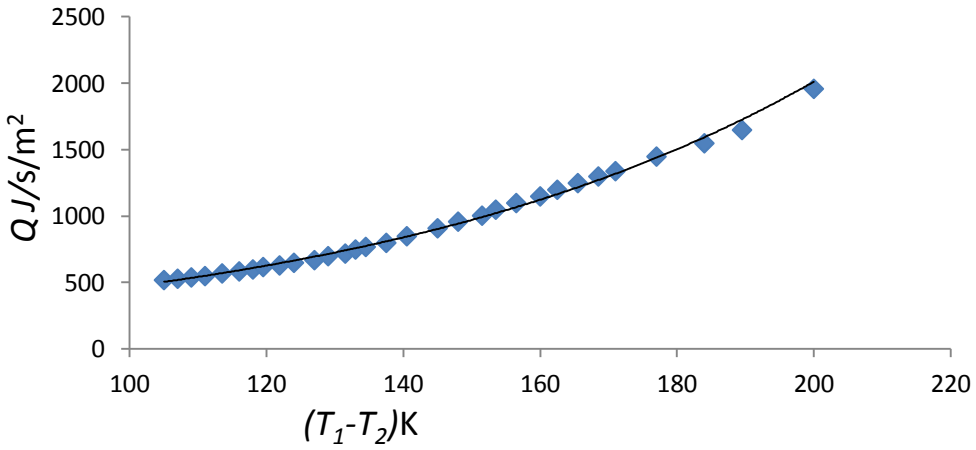

Figure 4.7: Heat loss rate for car solar reflector PTSC

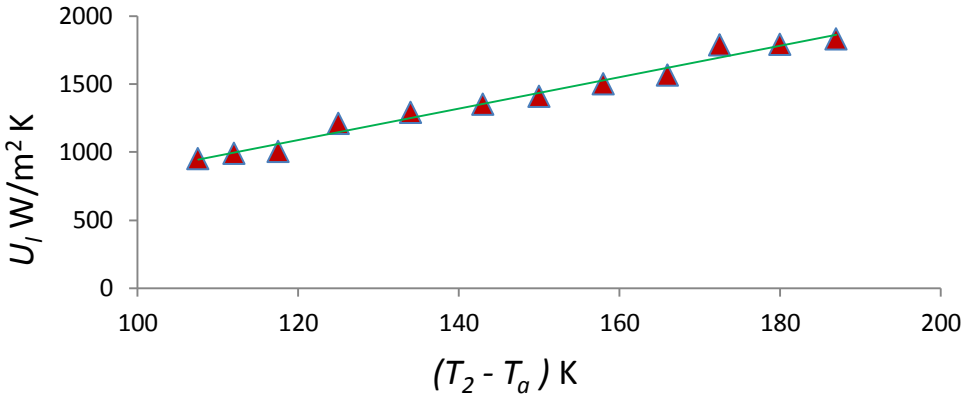

Figure 4.8: Overall heat loss coefficient for car solar reflector PTSC

Material III: Aluminium foil

Figure 4.9 shows heat loss rate by car solar reflector PTSC and Figure 4.10 shows

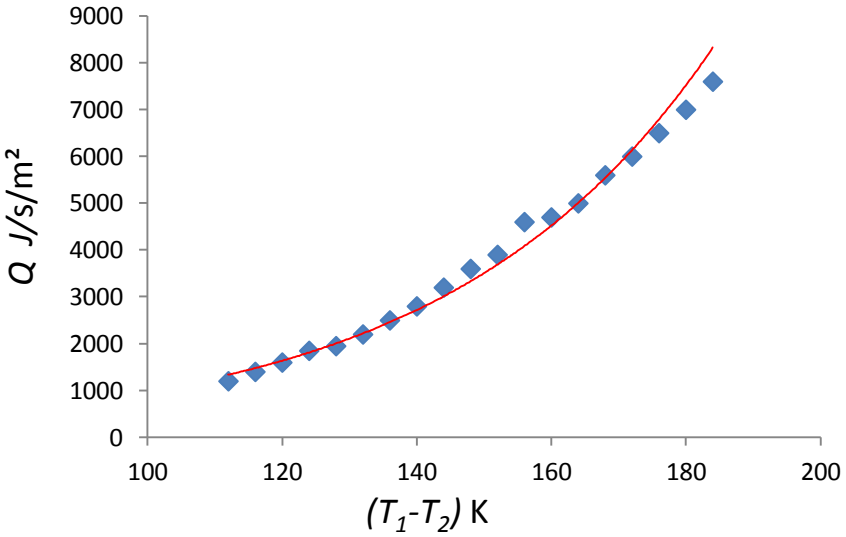

Figure 4.9: Heat loss rate for car solar reflector PTSC

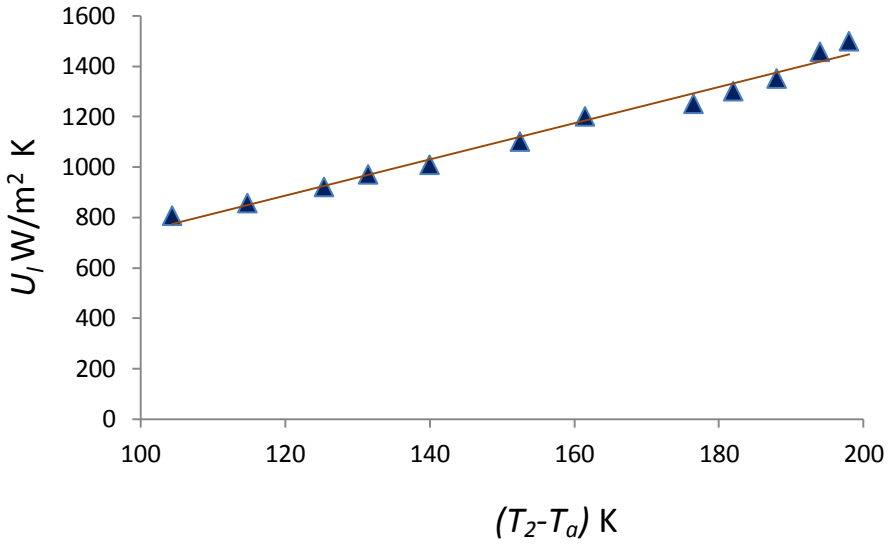

Figure 4.10: Heat loss coefficient for aluminium foil PTSC

The rate at which the fabricated collectors lost heat was obtained from Equation 4.20. The heat loss rates are seen to vary exponentially with difference in heat transfers out let temperature and the ambient temperature as shown in Figures 4.5, 4.7 and 4.9. The losses are seen to become more significant with increase in operational temperatures of the collectors. The heat loss rates for aluminium sheet PTSC, car solar reflector PTSC and aluminium sheet PTSC were obtained as 0.011 W/m^2, 0.014 W/m^2 and 0.025 W/m^2 respectively from Figures 4.5, 4.7 and 4.9.

The overall heat loss rates were obtained from Equation 4.21 and plotted against the difference between heat transfer's outlet temperature and the ambient. The heat loss coefficient was seen to increase with increase in operational temperatures of the collectors as seen in Figures 4.6, 4.8 and 4.10. The heat loss coefficients obtained for aluminium sheet PTSC, car solar reflector PTSC were 26.5 $W/m^2\ ^oC$, 291.8 $W/m^2\ ^oC$ and 16.7 $W/m^2\ ^oC$ as shown in the named figures.

4.10 Solar energy collection

4.10.1 Solar thermal energy collection characterization

The solar thermal energy absorbed by concentrator was obtained from Equation 4.11. Each concentrator was used for three days to produce steam. The amounts of heat energy collected depended on the intensity of solar normal beam from the sun, the reflectance of the material and the intercept factor among other factors.

Material 1: Aluminium sheet

In order to determine how the fabricated collectors were utilizing solar irradiance, each of the fabricated PTSC was used as described in Section 3.6. Variation of

temperatures, *TA* – Ambient temperature, *T1* – Heat transfer's fluid inlet temperature, *T2* – Heat transfer's fluid outlet temperature and *TC*– Collector chamber temperature were measured.

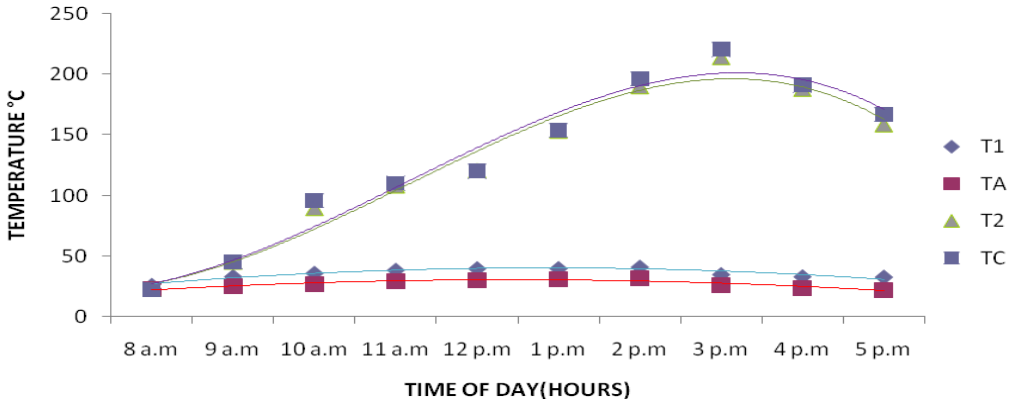

Figure 4.11: Temperatures for aluminium sheet PTSC on 18.9.2011.

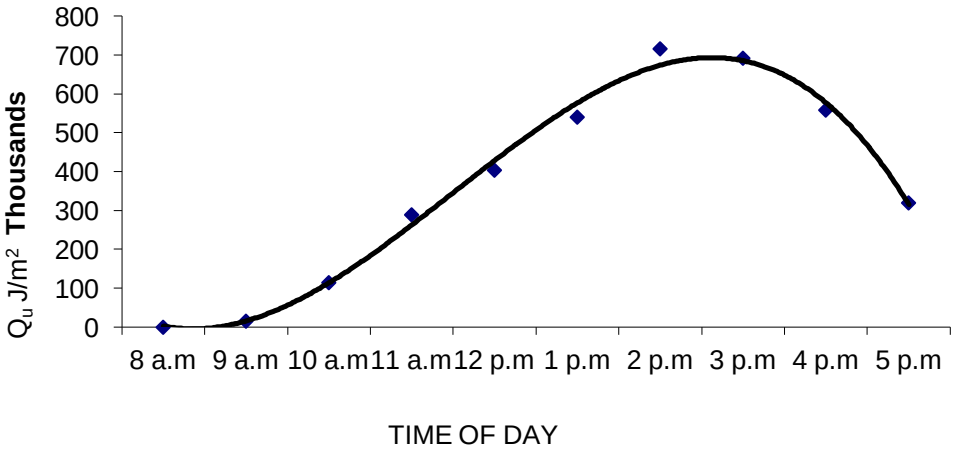

Figure 4:12: Energy collection against time of day.

The following measurements were taken: Mass flow rate as 9.9 kg/s, beam irradiance as 743.5 W/m^2 and pressure drop as 750000 Pa.

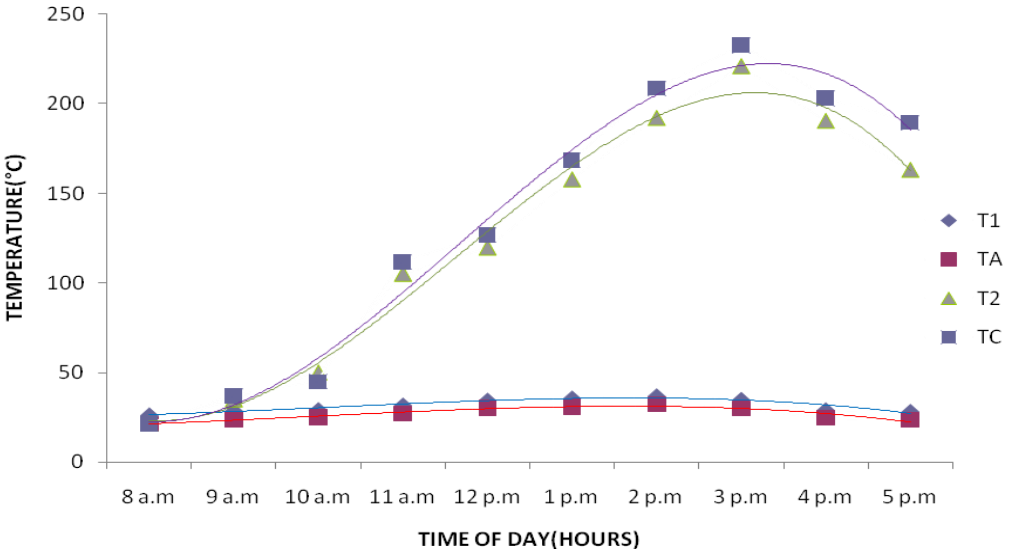

Figure 4.13: Temperatures for aluminium sheet PTSC on 19.9.2010.

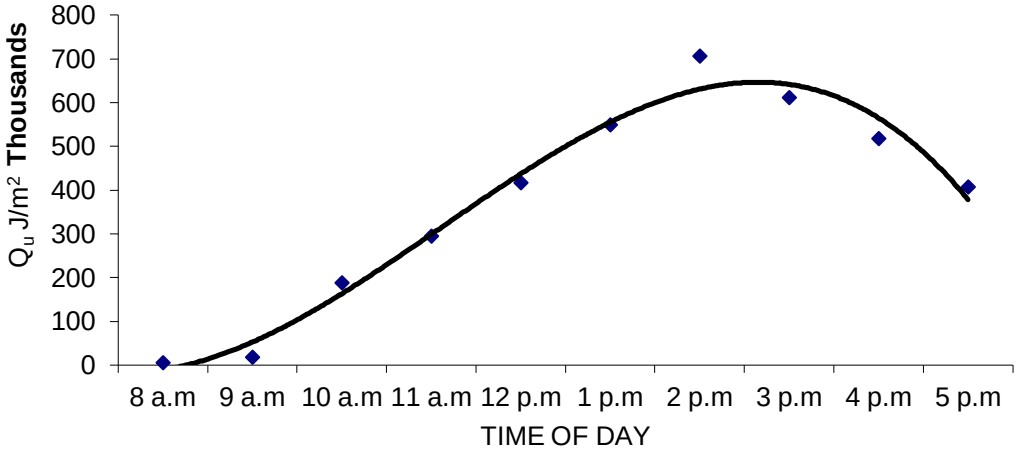

Figure 4.14: Energy collection against time of day.

The following measurements were taken: Mass flow rate as 10.1 kg/s, beam irradiance as 780 W/m^2 and pressure drop as 795000 Pa.

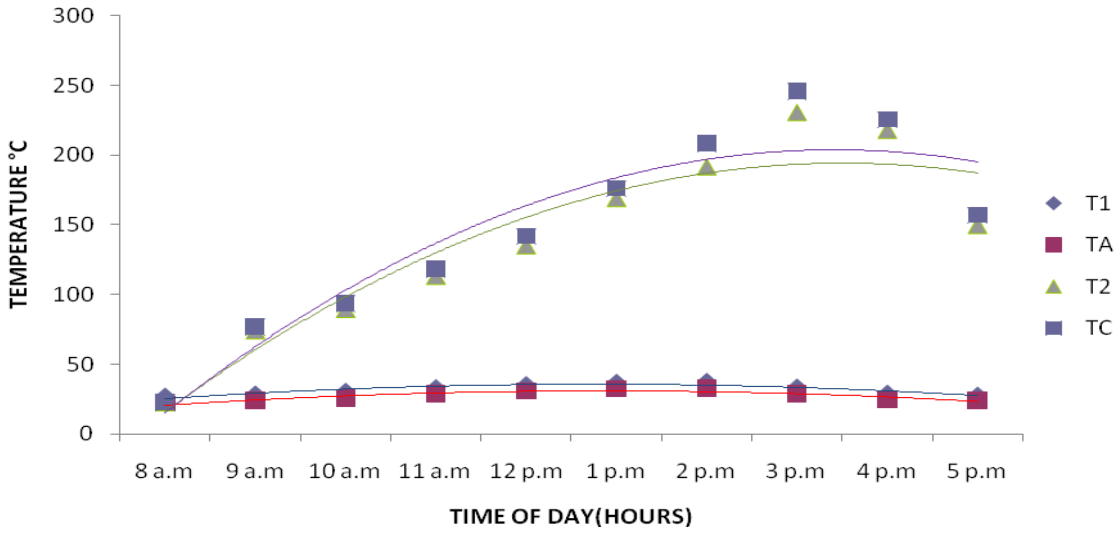

Figure 4.15: Temperatures for aluminium sheet PTSC on 20.9.2010.

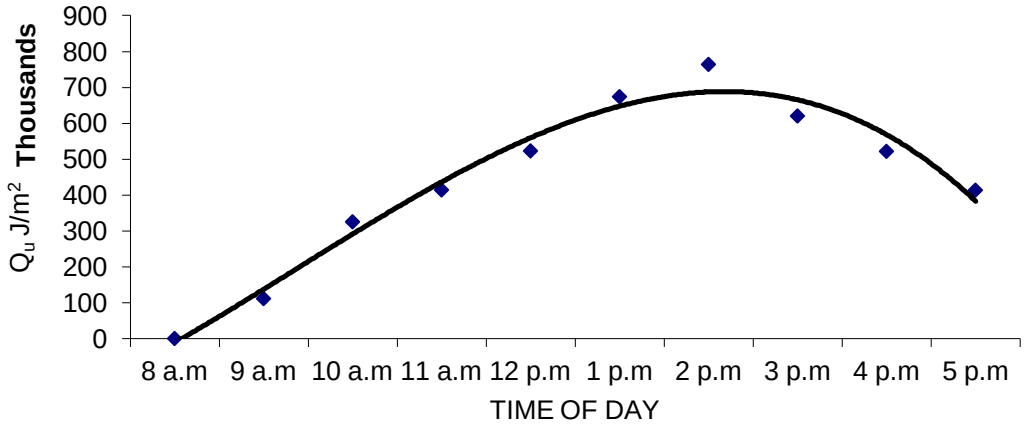

Figure 4.16: Energy collection against time.

The following measurements were taken: Mass flow rate as 9.7 kg/s, beam irradiance as 801.1 W/m^2 and pressure drop as 813000 Pa.

Material II: Car solar reflector

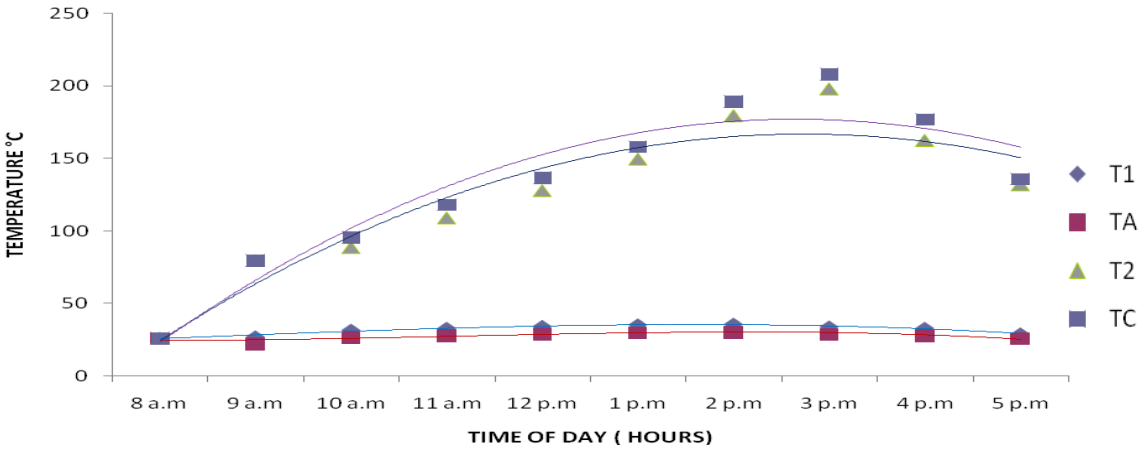

Figure 4.17: Temperatures for car solar reflector PTSC on 8.10.2010.

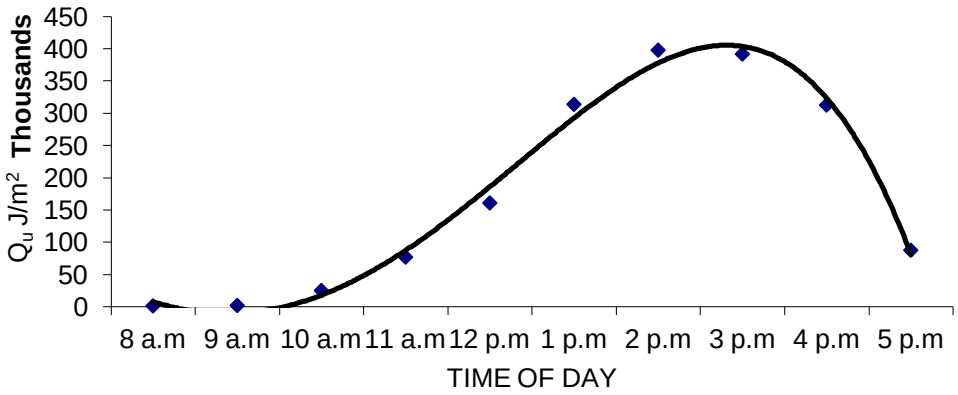

Figure 4.18: Energy collection against time of day for car solar reflector.

The following measurements were taken: Mass flow rate as 6.8 kg/s, beam irradiance as 520 W/m^2 and pressure drop as 500000 Pa.

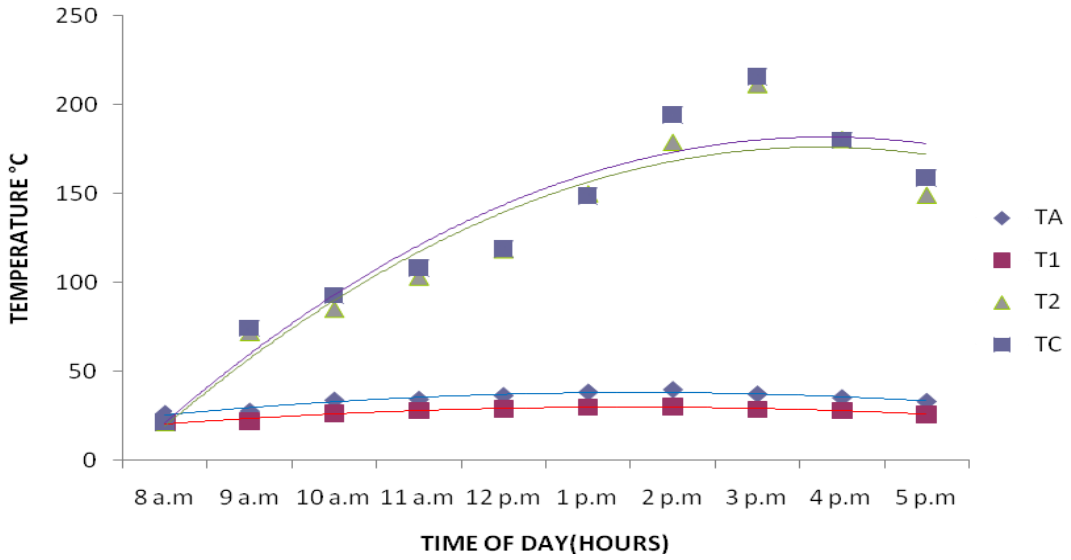

Figure 4.19: Temperatures for car solar reflector PTSC on 9.10.2010.

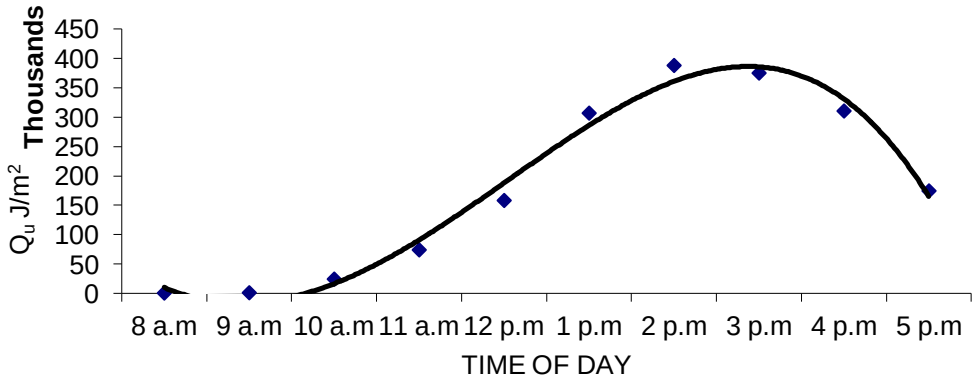

Figure 4.20: Energy collection against time of day for car solar reflector.

The following measurements were taken: Mass flow rate as 9.2 kg/s, beam irradiance as 580 W/m^2 and pressure drop as 584000 Pa.

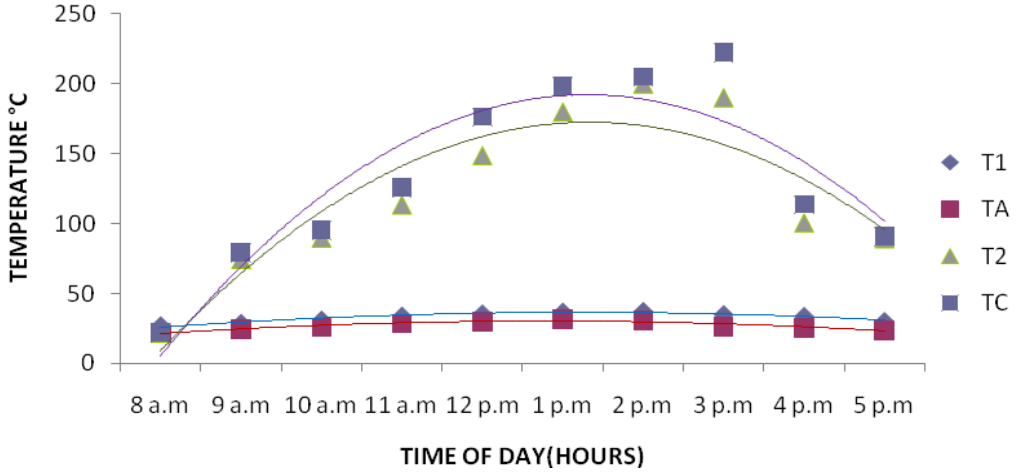

Figure 4.21: Temperatures for car solar reflector PTSC on 10.10.2010.

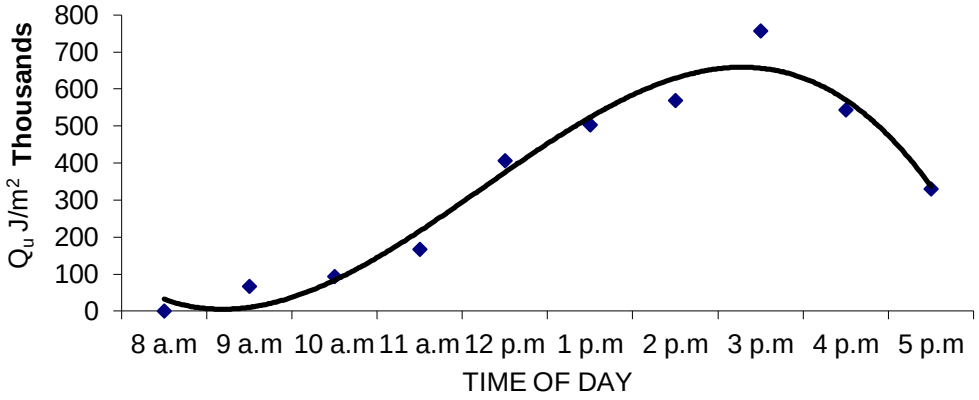

Figure 4.22: **Energy collection against time of day for car solar reflector.**

The following measurements were taken: Mass flow rate as 9.6 kg/s, beam irradiance as 700 W/m^2 and pressure drop as 685000 Pa.

Material III: Aluminium foil

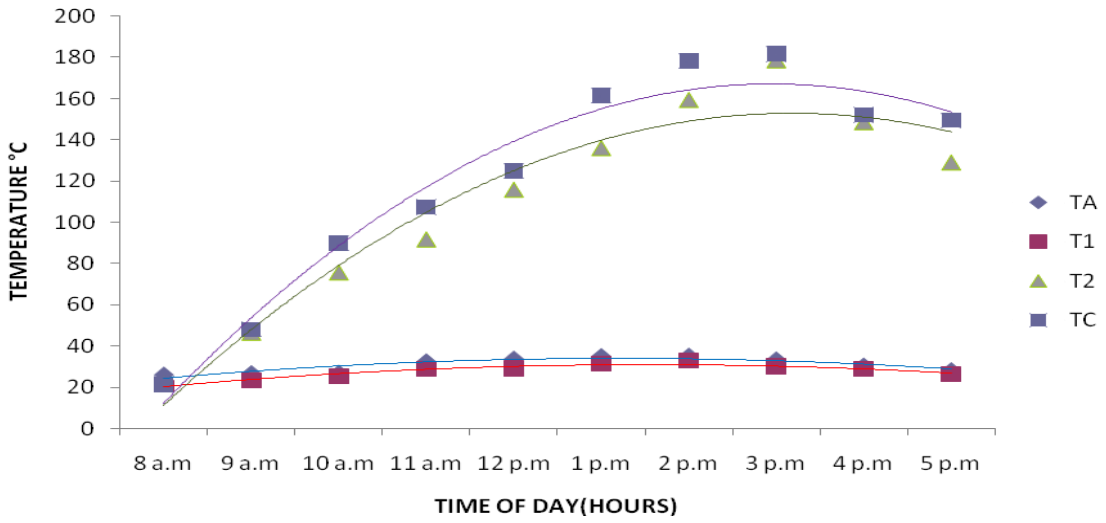

Figure 4.23: Temperatures for aluminium foil PTSC on 15.10.2010.

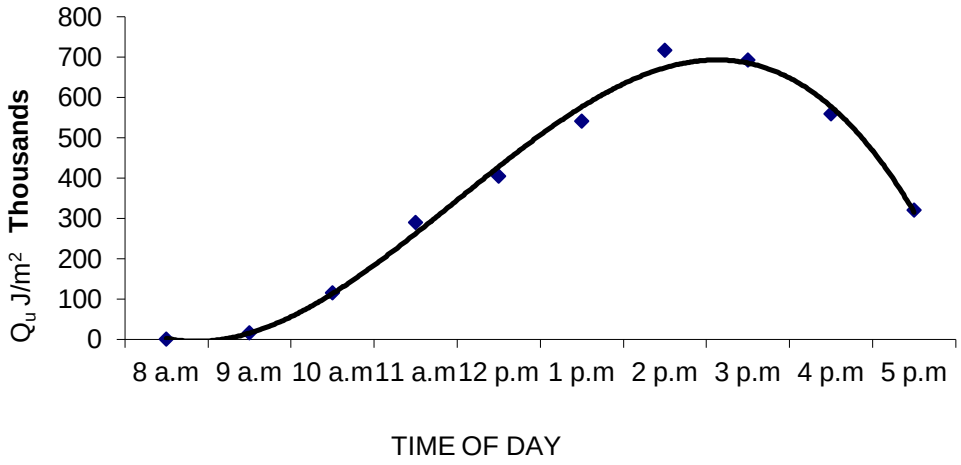

Figure 4.24: Energy collection against time of day for aluminium foil.

The following measurements were taken: Mass flow rate as 10.5 kg/s, beam irradiance as 795.2 W/m^2 and pressure drop as 800000 Pa.

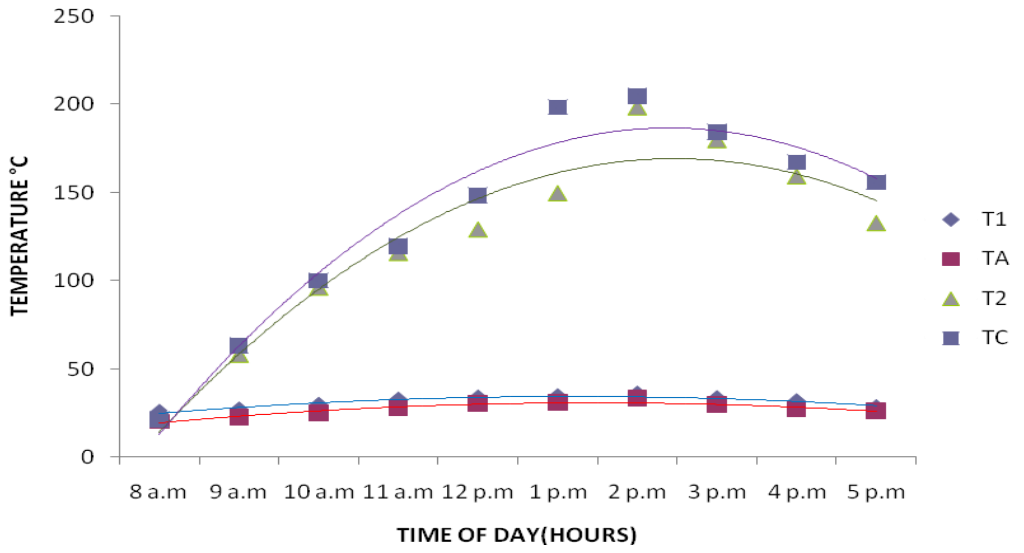

Figure 4.25: Temperatures for aluminium foil PTSC on 16.10.2010.

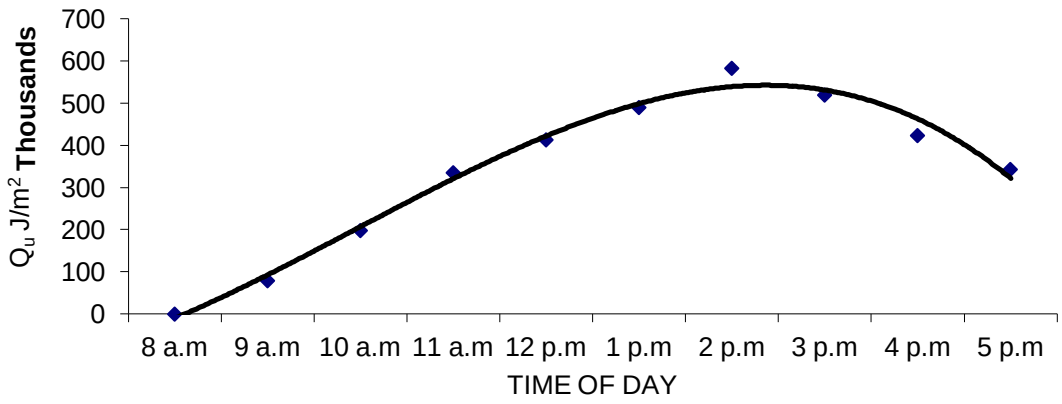

Figure 4.26: Energy collection against time of day graph for aluminium foil.

The following measurements were taken: Mass flow rate as 9.98 kg/s, beam irradiance as 770 W/m^2 and pressure drop as 871000 Pa.

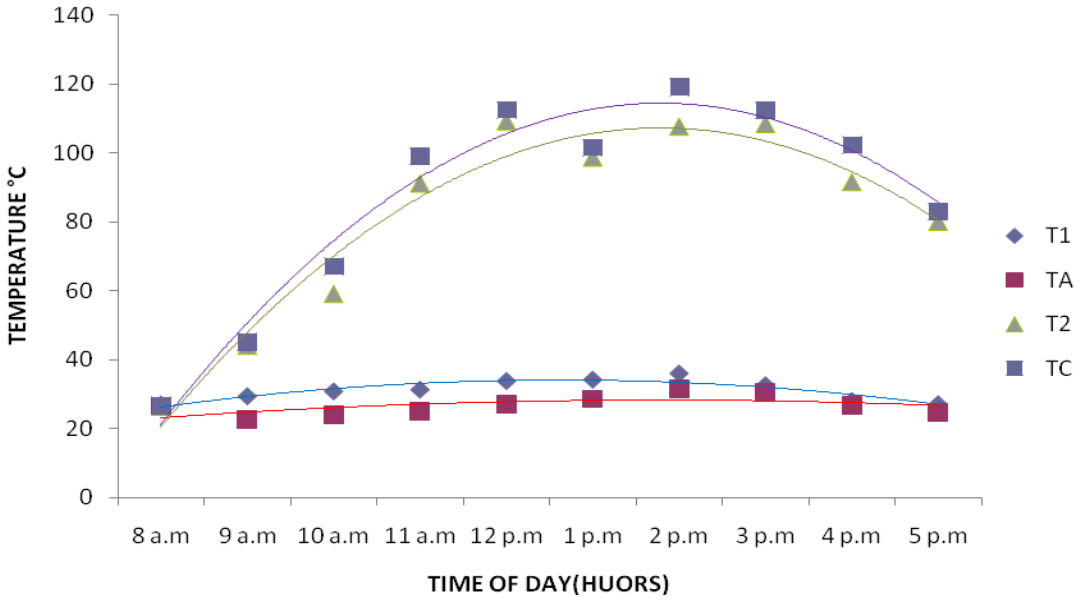

Figure 4.27: Temperatures for aluminium foil PTSC on 17.10.2010.

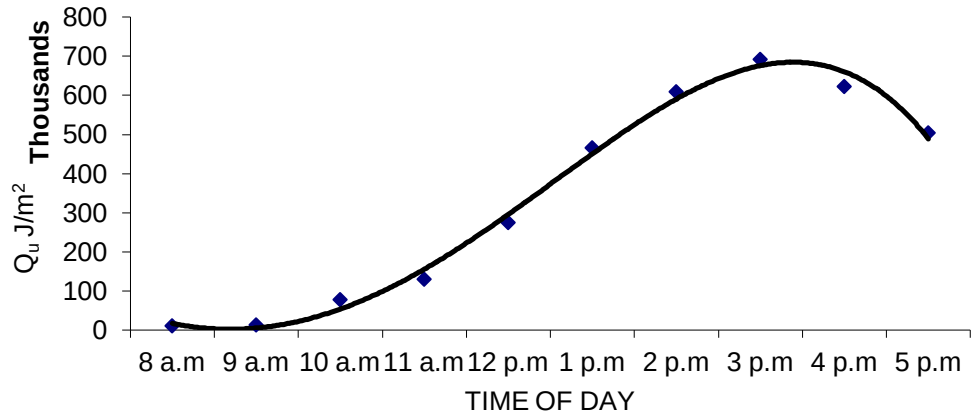

Figure 4.28: Energy collection against time of day graph for aluminium foil.

The following measurements were taken: Mass flow rate as 10.2 kg/s, beam irradiance as 848 W/m^2 and pressure drop as 982000 Pa.

The daily temperatures show a trend of increase from the morning to evening with a peak at midday when the solar intensity is at its highest. This is shown by graphs

4.11, 4.13, 4.15, 4.17, 4.19, 4.21, 4.23, 4.25 and 4.27. The chamber temperature *TC* is seen to be higher than the heat transfer liquid outlet *T2*. This is because the heat transfer fluid has a higher specific heat capacity compared to the air enclosed in collector chamber. The ambient temperature and the heat transfer's inlet temperature are close because the heat transfer liquid assumes temperature of the surroundings until the ambient temperature increases due to absorption of heat.

The collection of solar energy increased significantly at midday since it corresponds to the in increase of solar power intensity for a day. This is due higher proportion of normal solar beam from the sun to the collector at that time. Thereafter it decreases consistently due to the cooling lag experienced by the closed collector. Figures 4.15, 4.12, 4.14, 4.16, 4.18, 4.20, 4.22, 4.24 and 4.26, show that due to tracking in the N – S orientation the solar thermal energy obtained early in the morning and late in the afternoon show fair variability. This is ascertained by the presence of steady heating and cooling lag as observed in the above mentioned figures. Lower temperature differences between the heat transfer's outlet temperature and the ambient led to low yields of solar thermal energy as shown in Figures 4.17, 4.25, 4.27 and 4.31. The low temperature differences were caused by intermittent overcastting and during excessive heat losses by the collector. During the times when the beam component of incident solar radiation is low i.e. early in the morning and late in the afternoon, lower solar thermal energy output was observed. Steady increase in solar power intensity produced higher solar thermal power and higher efficiencies.

The capacity costs for the fabricated solar collectors were obtained as

2.26×10^{-7} kSh/J, 2.36×10^{-6} kSh/J and 2.84×10^{-4} kSh/J for aluminium sheet, car solar reflector and aluminium foil respectively. This is shown in Appendices G, H and I respectively. Tables H.1 and H.2 give the parameters that were used to find the capacity costs.

4.11 Fabricated PTSC pressure variations with temperature

In this section the solar thermal steam pressure that was shown by the pressure gauges as shown in plate A2 was plotted against temperature difference. This was done to characterize the concentrators in terms of solar thermal steam pressure output. The more the steam pressure the higher kinetic of the steam molecules and hence the higher the potential for higher power generation.

4.11.1 Solar thermal steam pressure characterization

Material I: Aluminium sheet

The commercial utilizability of a steam solar thermal power system depends on the steam power it can produce that can be converted into direct steam electricity generation or indirect power source. In this section variation of steam pressure as function of daily temperature difference is presented. The variation of steam pressure as a function of daily temperature difference for the three appropriate technologies fabricated PTSC are shown in Figure 4.29, 4.30 and 4.31.

Figure 4.29 shows the variation of steam pressure with temperature difference for the fabricated Aluminium sheet PTSC.

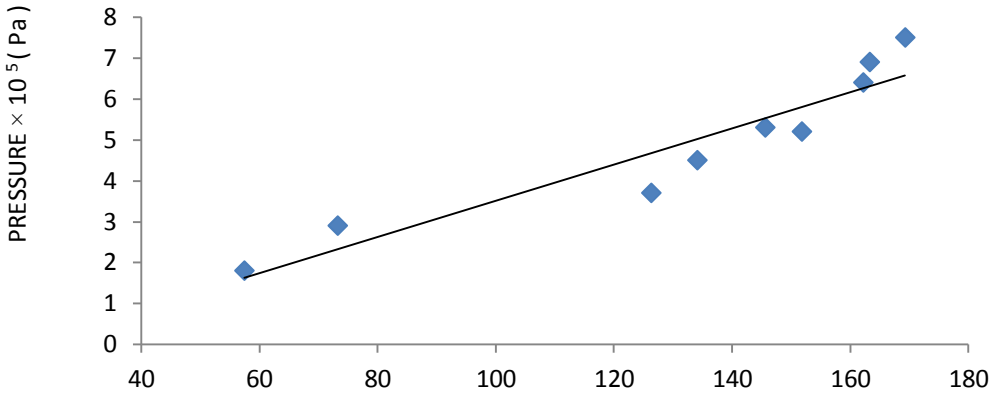

Figure 4.29: Variation of steam pressure with temperature difference graph for aluminium Sheet

Material II: Car solar reflector

The variation of steam pressure with temperature difference for the fabricated Car solar reflector PTSC is shown in Figure 4.30 .

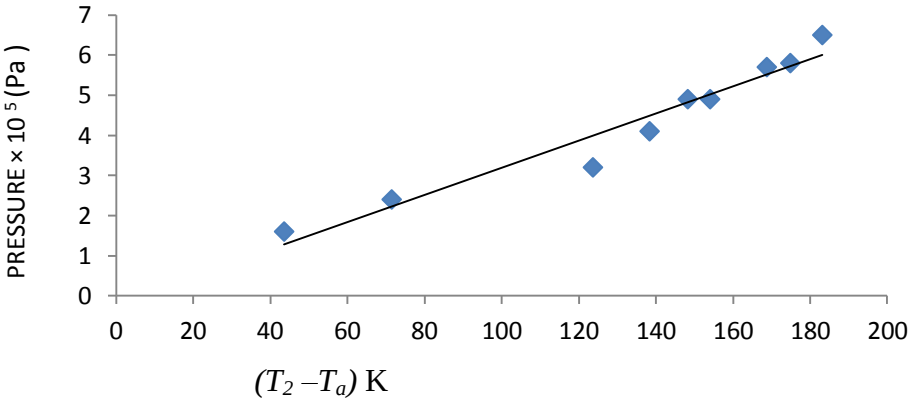

Figure 4.30: Variation of steam pressure with temperature difference for car solar reflector.

Material III: Aluminium foil

The variation of steam pressure with temperature difference for aluminium foil PTSC is shown in Figure 4.31.

From Figures 4.29, 4.30 and Figures 4.31 steam pressure produced by fabricated solar concentrators was observed to increase linearly with the temperature difference between the heat transfer's outlet temperature and the ambient. The higher the collectors heat transfer liquid's outlet temperature the higher the solar thermal steam output that was produced Increase in solar power intensity also produced an increase in solar thermal steam output. Overcast conditions scattered the incident solar beam from the sun. This caused a low proportion of normal solar beam to the collector hence a low solar thermal steam output.

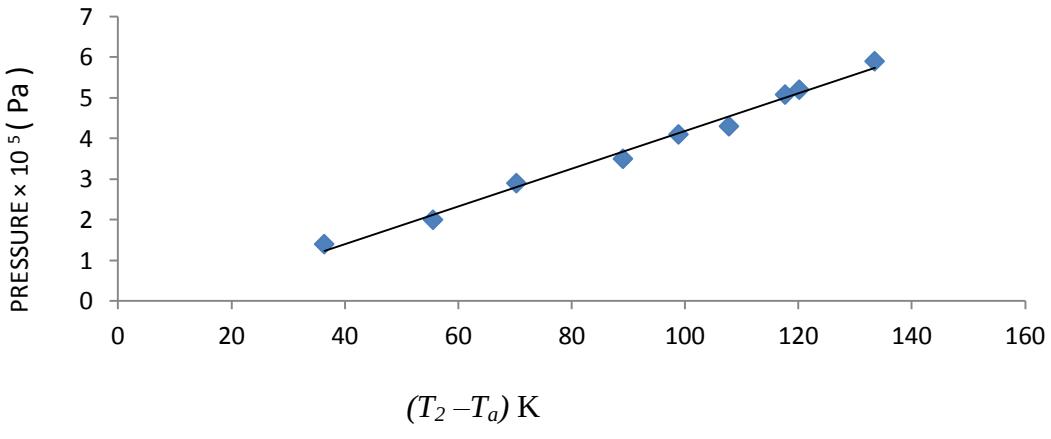

Figure 4.31: Variation of steam pressure with temperature difference graph for aluminium foil

CHAPTER FIVE

CONCLUSION AND RECOMMENDATIONS

In this study three prototype parabolic trough solar concentrators were designed fabricated and characterized using appropriate optical systems i.e. aluminium sheet, Car Solar reflector and Aluminium foil. Effective aperture area was 6.95m^2, collector area, 15.75m^2; focal length, 0.2; Collector length, 5.8 m; the absorber diameter, 0.0025m; concentration ratio, 128; aperture width, 1.2 m and its mass was 72.8 kg. The efficiencies for the closed PTSC were as follows: Aluminium sheet PTSC, 54.65 %, Car solar reflector 53.16% Aluminium foil, 49.26% which is lower than the efficiencies of Luz collector, 68 % , Euro trough, 65.2 % (Suhas, 1990) and Sky fuel parabolic trough, 73 % (Solar power, 2011). This is due to evacuation of absorber tube surroundings use of selective materials and automatic precise tracking systems that they use. The reflectances of the fabricated PTSC were as follows: aluminum sheet PTSC 0.83; car solar reflector PTSC 0.81; Aluminium foil PTSC 0.78; while those for documented concentrators were: aluminium for the Luz collector, 0.94 and Euro trough, 0.96 (John *et al*, 1991). The difference is as a result of the surface treatment of the optical systems, which improves their performance. The glass cover transmitivity of the 0.0025 m glass that was used in fabricated PTSCs was 0.8 while the Luz collector has 0.965 and the Euro trough has 0.95. This is because they use selective coatings. The fabricated PTSC systems costs were: Aluminum sheet PTSC; KSh 240,000 .00, Aluminium foil PTSC, KSh 220,805.00 and Car solar reflector PTSC; KSh 222,000.00. From the pressure values and efficiencies obtained the fabricated steam concentrators can be used to generate

power for a small industry in rural areas. The aluminium sheet PTSC produced the highest efficiency and would be the most appropriate for solar power generation, however the heat losses are significant and if reduced its performance would increase. Some solar energy collected by the fabricated concentrators was lost due to optical losses and thermal losses from the collector. However these can be kept at a minimum. In as much as the steam pressures increased with solar power intensity the weather can be unpredictable and hence reducing heat losses is the key to production of solar thermal power steam for large scale utility. The characterization techniques involved in this work involved use of local materials and the local technology that demystifies power production using parabolic trough solar concentrators in rural areas.

Apparatus such as Pyranometer, Pyrheliometer e.t.c which measure solar irradiance to a higher precision compared to the calorimetric method used in this work should be used. This is because the readings obtained from such measurements instruments provide a formidable basis for drawing conclusions. The apparatus were not used because they were not affordable.

An apparatus designed to measure intercept factor at various angles of the absorber would assist in design of concentrators and reflecting systems. This will enhance maximum utilization of incident solar flux. The calorimetric method used in this work is less accurate especially when variations of beam component are dominant.

The use of automatic tracking and photometrically aligning system as opposed to tracking system that was fabricated and manually effected here would improve the

quantity of solar energy collected per square meter and hence the efficiency of the steam generating system.

Lowering of the emissivity of appropriate paint used for the absorber would improve performance of fabricated collectors.

Evacuation of glass cover used for the fabricated concentrators would prevent heat losses by convection. This will ensure the solar energy in incident solar radiation beam is transferred to heat transfer fluid with minimum losses. Preventing heat losses from fabricated solar concentrators would improve the system's ability to deliver usable steam.

Some reflecting materials used in this work were highly prone to creasing e.g. Aluminium foil and Car solar reflector and hence means to make these appropriate materials as smooth as possible would enhance optical efficiencies of the systems. It is necessary to reduce the mass of the fabricated collectors by use of materials that are light and of high mechanical strength to make it more appropriate for rooftops.

REFERENCES

Alghoul M.A., Sulaiman, M.Y., and Wahab M.A. (2005), *Review of Materials for Solar Thermal Collectors*, Emerald Group Publishers, Malaysia. Pg. (200-207).

Aluminium Foil (2011), "Reflectance of Materials", http://www.alufoil.org/front-content html (6.1.2011, 11.00 p.m)

Arnold Muschet (2010), *Thermal Solar Plant*, Flowserve, Austria. Pg. (1-10)

Close D.J. (1988), *Flat Plate Solar Absorbers*, In: Engineering Section of Common Wealth Scientific and Industrial Research Organization, *Proceedings of a Workshop, May 21-27, Melbourne, Australia. Report E.D.7*

Dunkle R.V. and Divovosky P.W. (1961), *Thermal Radiation Tables and Applications, In:* Trans.ASME, Australia.76, 549.

Ecoworld (2010), "*Solar Thermal Energy*," http:// www.ecoworld.com/energy-fuels /solar Accessed 22/12/2009,3.00 a.m.

Ecoworld (2000), "*solar thermal power*," http://w.w.w.ecoworld.com/solarpower/solar steam html. Accessed 28.2.2011, 11.30 p.m

Energy (2000), "*World Bank Energy Report*," http:// www. undp. Org/seed/eap/publications /1999/19.99 a .Accessed 3/1/2010,5.30 p.m.

Hansson C.B. (1972), *Physical Data Book in SI Units*, Pergamon Press, Oxford. Pg. (5-20.)

Ganapathy V. (1994), *Steam Plant Calculations Manual,* Marcel Dekker, Inc., New York. *Pg.* (15-18).

Gillet W.B and Moon J.E. (1985), *Solar Collectors,* Reidel Publishing Company, Holland. Pg. (81-95).

John D, A. and William B.A. (1991), *Solar Engineering of Thermal Processes,* John Wiley & Sons Inc., Canada. Pg. (3-216, 330-379).

Kalogirou S, Lloyd S and Ward J.(1997), *Modeling, Optimization and Performance Evaluation of a Parabolic Trough Solar Steam Generation System,* Sol Energy, London. Pg. (49-59)

Kariuki M. (2006), *Fabrication and Characterization of an Effective Parabolic Solar heat Collector for Domestic Hot Water Supply,* Msc. Theses, Jomo Kenyatta University of Agriculture and Technology, Nairobi, Kenya. Pg. (21-51).

Parabola(2007), " *Trough Geometric Design*. http://www.bilfoster/2007/112/en. Accessed 24.3.2010, 5.30 a.m

Power from the Sun (2009), "*Science Encyclopedia*," www.Power from the sun. Net/chapter 2.20/3/2010,2.00 a.m.

Price H, Lufert E and Kearney D, (2010), *Advances in Parabolic Trough Solar Technology,* Sol Energy-T ASME, London. Pg.(109-125).

Rabl Ari, (1985), *Active Solar Collector and their Applications,* Oxford University Press, London. Pg. (15-230).

Rai G.D. (1987), *Solar Energy Utilization,* Hama Publishers, NewDehli. Pg. (1-19, 160-190).

Renewable Energy (2008),''*Natural Renewable Energy Laboratory*", http://www.Nrel/.Govl. Accessed 25.2.2010, 6.00 a.m

Solar taskforce Report (2006), "*Western governors Association, Clean and Diversified Energy initiative*," http://www.West gov.org /wga/initiatives/cdeac/solar.Acessed 28/4/2010,10.45 p.m.

Solar Concentrators (2011), "Concentrating solar power Research", "http://www.nrel.gov/csp/lab-capabilities html. Accessed 13/8/2011, 6.30 a.m.

Solar Power (2011), ''*Solar Thermal Power Research*", ''http://www.energysaving.nu/solarenergy/thermal.shml. Accessed 23/9/2011, 11.20 p.m.

Solar Steam Power, (2011), "*Parabolic Steam Power*", ''http;//www.nrel.gov/csp/troughnet/market-economics-asses.html. Accessed 4/3/2011, 1.46 p.m

Solar Thermal Resource (1999), "*Solar Energy Applications*," http;/www.energy/env……../p. Accessed 29/6/2010, 5.30 p.m

Solar Thermal Energy (2005), "*Wikipedia Free Encyclopedia*," http;//en.wikipedia.org /wiki / solar thermal .Accessed 12.12.2009, 10.30 a.m.

Solar Thermal Power Report (2010), "*Market Research Report*," http://www.market research.com/…./2526650.html .Accessed 31.3.2010, 1.00 p.m.

Solar and Wind Energy Resource Assessment (2006), "*Renewable Energy*", http:// www.swera.unep.net. UNEP/Grid-Sioux falls .Accessed 5.5.2010, 11.45 p.m.

Solar Radiation (2011),"*Transmittance*" , htpp://almashriq.hlo.no/Lebanon/600/614/01-09.

Suhas P.S. (1992), *Solar Energy.* Tata Mc Graw Hill Publishing Co. Ltd, Newdehli. Pg. (7- 80).

SWERA (2010), "*Renewable Energy Resources*" , http://www.swera.com/renewableenergy/powersource.research.com/..Accessed 28.2.2011, 11.30 p.m

Twidel D.S., John W., and Anthony D.W. (1986), *Renewable Energy Resources,* ELBSLE and F.N Spon Ltd, London. Pg. (17-45)

Wikipedia Free Encyclopedia (2011), "Solar Thermal Energy Processes", "http://www wikipedia.org/wiki/ solar thermal. Accessed 27.1.2010, 11.30 a.m

World Energy Resources (2002), "Fossil Fuels" .http://undp.org/seed/eap/publications/2001/html. Accessed 13.4.2010, 10.50 p.m

APPENDICES

APPENDIX A: Fabricated solar concentrator photographs

Plate A 1: Photograph of the prototype parabolic solar concentrator.

Plate A 2: Open loop collector testing system

Plate A 3: Heat exchanger and inlet system of water for collection

Plate A 4: measurement of Intercept factor after some data collection by calorimetric method.

APPENDIX B: Projected solar thermal energy utilization for aluminium sheet concentrator.

Suppose 10 liters of water at inlet temperature of 25 ºC is required for industrial process heat to provide steam at a temperature of 150 ºC, the collector area that would be required to meet the steam demand can be determined as follows:-

The load per day was obtained as the sum of heat required to raise temperature of liquid water from 25 ^{o}C to boiling point, latent heat of vaporization of water and the heat that was required to raise the temperature of steam by 50 ^{o}C.

The load per day was obtained as 26970 kJ/day, and the load per year 9.778×10^{6} k J/yr.

The latent heat of vaporization, *Lv* of steam was presented as: L_V=2.26 x 10^{6} J/kg °C (Hanson, 1972).

Transmittance absorptance product of glass used was 0.8, net annual load would be Obtained as the product of annual load and absorptance transmittance for glass and was 7.82×10^{6} kJ/year.

Average radiation on collector plane was found as 852.7 W/m^2 but only 80 % is transmitted by cover system. Therefore effective solar intensity was 682.16 W/m^2

Annual average for 10 hour actual collection neglecting overcast conditions would be obtained from Equation B.1 as 50.112 W/m^2.

$$Q_{u=} \frac{A_a}{A_c} F_R[I_b \rho \gamma \langle \alpha\tau \rangle - U_l (T_m - T_a)] \quad \text{(B.1)}$$

$Q_{U,}$ annual collection in 365 days of the year would be obtained as 6.58 x 10^{8} J/m^2/yr.

$$CA = \frac{L}{Q_u} \quad \text{(B.2)}$$

Where L is the load and Q_u is the useful heat gain by the collector.

Using Equation B.2 the collector area was obtained as 11.88 m^2.

The size of the receiver, D that would intercept the entire solar image could be determined by of equation below (John *et al*, 1991).

$$2r_r \sin 0.267 = \frac{a \sin 0.267}{\sin \emptyset_r} \quad \text{(B.3)}$$

Where r_r is maximum mirror radius and a is aperture.

The geometry of the parabola is defined by its aperture, D and focal length, f. Total solar energy incident on the mirror was obtained as 960 J/m^2 from the following equation (John *et al*, 1991).

$$\frac{1}{4}\pi D^2 I_b \quad \text{(B.4)}$$

APPENDIX C: Projected solar thermal energy utilization for car solar reflector concentrator

Suppose 10 liters of water at inlet temperature of 25 ºC is required for industrial process heat to provide steam at a temperature of 150 ºC , the collector area that would be required can be determined as follows:-

Load per day was obtained as 26970 kJ/day and the load per year as 9.778×10^6 kJ/yr.

Transmittance absorptance product of glass used was 0.8; net annual load would be obtained as 782×10 J as shown in appendix B.

Average radiation on collector plane was found as 852.7 W/m^2 but only 80 % was effective due glass cover transmittance hence effective radiation was obtained as 682.2 W/m^2.

Annual average for daylight hour is 10 hour neglecting overcast weather actual collection would be obtained from equation B.1 as 50.632 W/m^2.

$Q_{u,}$ annual collection was obtained as 6.4×10^5 J/m^2/yr.

The collector area that would be required to harness this energy was obtained as 12.21 m^2 from equation B.2.

APPENDIX D: Projected solar thermal energy utilization for aluminium foil Concentrator

Suppose 10 liters of water at inlet temperature of 25 ºC is required for industrial process heat to provide steam at a temperature of 150 ºC. The collector area that would be required to provide the steam power would be;-

Load per day was obtained as 26790 kJ/day as shown in appendix B

Load per year was obtained as 9.778×10^6 kJ/yr.

Average transmittance of glass used was 0.8, and hence the effective net annual load was obtained as 7.82×10^6 kJ/yr.

Average radiation on collector plane was found as 852.7 W/m^2 but only 80 % is transmitted by cover system so that the available solar power intensity was determined as 682.2 W/m^2.

Annual average for daylight hour is 10hr. actual collection would be obtained as 47.48 W/m^2 from equation B.1.

$Q_{U,}$ annual collection neglecting overcast weather was obtained as 6.24×10^5 J/m^2/yr

Collector area was obtained as = 12.53 m^2 from Equation B.2.

The size of the receiver that would intercept the entire solar image is given by Equation B.4.

APPENDIX E: Summary of Characteristics of the Fabricated Prototype Parabolic Trough Solar Concentrators.

Collector flow factor

Table E.1 shows the collector flow factors obtained for fabricated concentrators. These values were obtained by use of Equation 4.18.

Table E.1: Collector flow factor

PTSC	COLLECTOR FLOW FACTOR
Aluminium sheet	1.50
Car solar reflector	1.42
Aluminium foil	1.52

Collector heat removal factor

Table E.2 shows how the heat removal factor for the fabricated solar concentrators compared. The collector heat removal factor was obtained from Equation 4.16. When the performance of the concentrator is high the collector heat removal factor also increased. This is evident from Figure 4.2 where aluminium sheet solar concentrator has the highest efficiency and also has highest heat removal factor.

Table E.3 shows a summary of collector efficiency factors for the fabricated solar concentrators. The collector efficiency factor was obtained from Equation 4.17. This factor is used in design of concentrator since it has higher values in better performing concentrators.

Table E.2: Collector heat removal factor

PTSC	COLLECTOR HEAT REMOVAL FACOR
Aluminium sheet	0.90
Car solar reflector	0.53
Aluminium foil	0.56

Table E.3: Collector efficiency factor

PTSC	COLLECTOR EFFICIENCY FACTOR
Aluminium sheet	0.64
Car solar reflector	0.60
Aluminium foil	0.56

APPENDIX F: Capacity cost for aluminium sheet solar concentrator

Average solar thermal energy collected per day was obtained using Equation 3.4 as 2.90×10^9 J.

Average solar thermal steam energy absorbed per year was also obtained as

1.06×10^{12} J.

Total Aluminium sheet system cost was KSh 240000.00.

Average collector operating temperature of aluminium sheet collector was 198.4 ^oC.

Average annual direct normal radiation at site was obtained as 752 W/m^2 from Section 4.5. Capacity for the collector was obtained using the equation below as 2.26×10^{-7} KSh/J.

APPENDIX G: Capacity cost for car solar reflector solar concentrator

The cost of steam power generated per joule by car solar reflector PTSC was obtained using Equation 3.4 as 2297866.361J:

Average thermal steam energy absorbed per year was obtained as 8.38×10^{9}J

Total Car solar reflector PTSC system cost was KSh 222000.00.

Average collector operating temperature for the fabricated collector was 179.8 ^{o}C.

Average annual direct normal radiation at site was obtained as 520 W/m^{2} from Section 4.5.

Capacity cost was obtained using Equation F.1 as 2.36×10^{-6} Ksh/J.

APPENDIX H: Capacity cost for aluminium foil solar concentrator

The cost of steam power generated per joule by fabricated Aluminium foil PTSC was obtained using Equation 3.4.

Average solar thermal steam energy absorbed per day was obtained as 2128753.147 J.

Average solar thermal steam energy absorbed per year was obtained as 776994898.7 J.

Total Aluminium foil collector system cost was obtained as KSh 220805.00.

Average collector operating temperature for this collector was 157.5 ^{o}C.

Average annual direct normal radiation at site was obtained as 800 W/m^2 from Section 4.5.

Capacity cost was obtained from Equation F.1 as 2.84 x 10^{-4} Ksh/J.

In summary the systems cost were as follows:

Table H.1: Collector system costs

PTSC	COST
Aluminium sheet	KSh 240000.00
Car solar reflector	KSh 222000.00
Aluminium foil	KSh 220000.00

Table H.2: Capacity cost of fabricated collectors

PTSC	CAPACITY COST
Aluminium sheet	2.26×10^{-7} KSh/J
Car solar reflector	2.36×10^{-6} KSh/J
Aluminium foil	2.84×10^{-4} KSh/J

APPENDIX I: Radiation Tables (Dunkle and Divovosky, 1961)

Table I.1: Spectral distribution of terrestrial beam radiation at air mass 2.

Energy band fi-(fi+1)	Wavelength ,µm	Midpoint wavelength , µm
0.00-0.05	0.00-0.434	0.402
0.05-0.10	0.434-0.479	0.458
0.10-0.15	0.478-0.517	0.498
0.15-0.20	0.517-0.557	0.537
0.20-0.25	0.557-0.595	0.576
0.25-0.30	0.595-0.633	0.614
0.30-0.35	0.633-0.670	0.652
0.35-0.40	0.670-0.710	0.690
0.40-0.45	0.710-0.752	0.730
0.45-0.50	0-.752-0.799	0.775
0.50-0.55	0.799-0.845	0.820
0.55-0.60	0.845-0.894	0.869
0.60-0.65	0.894-0.975	0.923
0.65-0.70	0.975-1.035	1.003
0.70-0.75	1.035-1.101	1.064
0.75-0.80	1.101-1.212	1.170
0.80-0.85	1.212-1.310	1.258

0.85-0.90	1.310-1.603	1.532
0.90-0.95	1.603-2.049	1.689
0.95- 1.0	2.049-5.000	2.292

Table I.2: Temperature dependent midpoint wavelengths

F_o-λT	λT,μmK	λT at midpoint
0.05	1880	1660
0.10	2200	2050
0.15	2450	2320
0.20	2680	2560
0.25	2900	2790
0.30	3120	3010
0.35	3350	3230
0.40	3580	3460
0.45	3830	3710
0.50	4110	3970